European Journal of Medicinal Chemistry 53 (2012) 176–189

Contents lists available at SciVerse ScienceDirect

European Journal of Medicinal Chemistry

journal homepage: http://www.elsevier.com/locate/ejmech

Original article

Synthesis, characterization, antimicrobial activities and QSAR studies of some 10a-phenylbenzo[*b*]indeno[1,2-*e*][1,4]thiazin-11(10a*H*)-ones

Satbir Mor [a,*], Preeti Pahal [a], Balasubramanian Narasimhan [b]

[a] *Department of Chemistry, Guru Jambheshwar University of Science and Technology, Hisar 125001, Haryana, India*
[b] *Faculty of Pharmaceutical Sciences, Maharshi Dayanand University, Rohtak 124001, India*

ARTICLE INFO

Article history:
Received 7 December 2011
Received in revised form
29 March 2012
Accepted 29 March 2012
Available online 19 April 2012

Keywords:
1,4-Benzothiazines
2-Aminobenzenethiols
Antibacterial
Antifungal

ABSTRACT

A series of 10a-phenylbenzo[*b*]indeno[1,2-*e*][1,4]thiazin-11(10a*H*)-ones (**3**) has been synthesized and tested for their antimicrobial activity. The antimicrobial evaluation data indicated that compounds, **3b**, **3d**, **3k** and **3m** exhibited very promising antibacterial activity and the compounds **3b** and **3k** exhibited notable activity, almost comparable to penicillin for *Staphylococcus aureus* and *Bacillus subtilis* respectively. The derivatives **3g** and **3l** exhibited high antifungal activity. Moreover, antibacterial activities were more prolific than antifungal activity. The QSAR studies indicated the importance of topological parameters, Kiers second order molecular index ($\kappa\alpha_2$) and molecular connectivity index (χ) in describing the antibacterial activity and electronic parameters, the energy of highest occupied molecular orbital (HOMO) and the dipole moment (μ) in describing the antifungal activity.

1. Introduction

Heterocycles containing nitrogen and sulphur as heteroatoms undoubtedly constitute an important class of highly applicable bioactive molecules because of their interesting biological activities and uses as key structural motif for the synthesis of various natural products of pharmaceutical interest [1]. Amongst them a large number of thiazine ring containing drugs with versatile type of applications are being used clinically. These compounds have immense chemotherapeutic importance as vasodilator [2], antidiabetic [3,4], antiemetic [5], antiarrhythmic [6,7], antitumoral [8], anti-inflammatory [9], antidepressant [10], antibacterial [11] activities, etc. These compounds are also reported as calcium channel blockers [12,13], phosphodiesterase inhibitors [14], 5-HT3 antagonists [15], anti-HIV agents [16], cytostatic agents [17], Na^+/H^+ exchange inhibitors [18], antithrombotic [19] and lipoxygenase inhibitors [20]. The basic unit present in mammalian red hair and feather is 1,4-benzothiazine nucleus [21]. Benzothiazines also find uses as steel corrosion inhibitors [22], K_{ATP}-Channel Openers [23], antioxidants [24], dyes [25] and photosensitizers [26].

A recent review by Brown et al. [27] provides an excellent account of the chemistry of benzothiazines and their related compounds. The importance and utility of benzothiazine derivatives have led to the development of various synthetic routes i.e. the reaction of 2-aminobenzenethiols with alkynes [28], α-halo ketones [29], α-halo esters [30], oxidative cyclocondensation of 2-aminobenzenethiols with 1,3-dicarbonyl compounds using dimethyl sulfoxide [31,32], etc. The most convenient method for the synthesis of these compounds involves the treatment of dinucleophiles with suitable carbon fragments under appropriate reaction conditions, e.g., reaction of α-halo ketones with 2-aminothiophenol and its derivatives. A relatively unexplored heterocyclic ring system, with respect to both synthesis and biological activity is indenobenzothiazine derivatives [33].

Quantitative structure–activity relationship (QSAR) is one of the most important areas in chemometrics, and is a valuable tool that is used extensively in drug design and medicinal chemistry. Once a reliable QSAR model is established, we can predict the activities of molecules, and know which structural features play an important role in biological processes [34].

As part of our program aimed at synthesis and biological evaluation of heterocyclic compounds containing nitrogen and sulphur as heteroatoms and in view of the continuous interest for new antimicrobial agents we report herein, the synthesis, characterization, antimicrobial activities (antibacterial and antifungal) and

* Corresponding author. Tel.: +91 1662 263397; fax: +91 1662 276240.
E-mail address: satbir_mor@yahoo.co.in (S. Mor).

0223-5234/$ – see front matter © 2012 Elsevier Masson SAS. All rights reserved.
doi:10.1016/j.ejmech.2012.03.054

QSAR studies of some 10a-phenylbenzo[*b*]indeno[1,2-*e*][1,4]thiazin-11(10a*H*)-ones (**3**).

2. Results and discussion

2.1. Chemistry

The α-halo ketones chosen to carry out the reaction were 2-bromo-2-arylindan-1,3-diones (**1**) which were obtained by bromination of 2-arylindan-1,3-diones [35] which, in turn, were prepared by condensation of phthalide with benzaldehyde/p-substituted benzaldehyde in the presence of an alkoxide and ester in high yields [36,37]. The 5-substituted-2-aminobenzenethiols needed for the purpose were synthesized in good yields by base catalyzed hydrolytic fission of 6-substituted-2-aminobenzothiazoles as per literature procedures [38–40]. The condensation of 2-bromo-2-arylindan-1,3-diones with 2-aminobenzenethiols/5-substituted-2-aminobenzenethiols in boiling ethanol furnished the corresponding 10a-phenylbenzo[*b*]indeno[1,2-*e*][1,4]thiazin-11(10a*H*)-ones (**3a**–**3p**) in excellent yields (72–85%) (Scheme 1).

The structures of all the newly synthesized compounds were established on the basis of spectral and analytical data. The IR spectra of compounds **3a**–**3p** displayed characteristic absorptions in the regions 1696–1682 cm^{-1} and 1615–1596 cm^{-1} corresponding to aromatic >C═O (conjugated keto group in a five membered ring) and C═N groups respectively [41,42]. The ^1H NMR spectra of **3a**–**3p** exhibited at lowest field one proton doublet in the region δ 9.03–9.19 which can be easily assigned to C_6–H of the benzothiazine moiety because of its proximity to the N-atom on analogy with a similar proton in quinolines [43,44]. Next, towards the higher field was located a one proton doublet, in the region δ 7.82–7.95 assigned to C_1–H. The deshielding of this proton relative to other protons (C_2–H, C_3–H and C_4–H) of indanone benzene ring is due to the anisotropic effect of the contiguous C_{11}-carbonyl group. On moving towards higher field, the compounds **3a**, **3e**, **3i** and **3m** exhibited doublet in the region δ 7.07–7.17 due to C_8–H and C_9–H with coupling constant (*J*) ranging from 8.1 to 8.4 Hz which is in accord with ortho coupling. However, the compounds **3b**, **3c**, **3d**, **3f**, **3g**, **3h**, **3j**, **3k**, **3l**, **3n**, **3o** and **3p** displayed doublet in the region δ 6.62–7.21 due to C_9–H with coupling constant (*J*) ranging from 2.0 to 2.8 Hz which may arise due to meta coupling since C_8 carry substituents in all these derivatives. At the higher field of spectra, in the aromatic region was located one proton doublet in the region δ 6.46–6.94. The most suitable contender for this proton seems to be of $C_{2'}$–H, which due to the orthogonal disposition of C_{10a}-phenyl group lies in the shielding zone of the C_{11}-carbonyl group. The perpendicular disposition of C_{10a}-phenyl group may arise due to steric interaction between electrons of $C_{6'}$–H bond and lone pair of electrons on sulphur atom on one side and electrons of $C_{2'}$–H bond and lone pair of electrons present on oxygen atom of C_{11}-carbonyl group on the other side. The remaining aromatic and aliphatic protons displayed signals in their characteristic regions. Further, the ratio of aromatic to aliphatic protons was found satisfactory (vide experimental). The ^{13}C NMR spectra of benzothiazine derivatives **3a**–**3p** exhibited in most downfield region at δ 182.34–184.92 which can be easily assigned

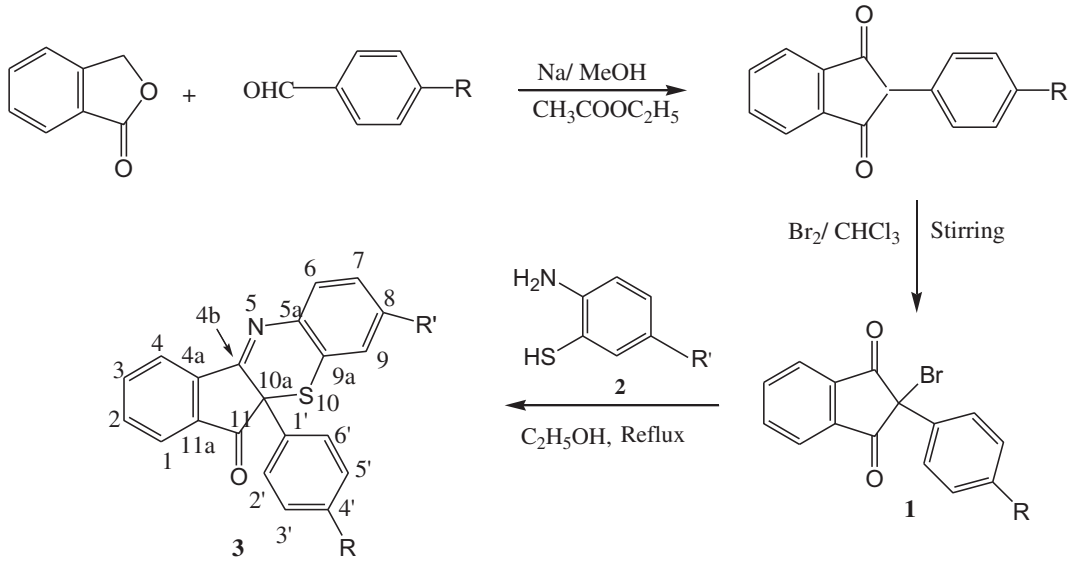

3a: R=R'=H
3b: R= H, R'= CH_3
3c: R= H, R'= OCH_3
3d: R= H, R'= Br
3e: R= CH_3, R'=H
3f: R= CH_3, R'= CH_3
3g: R= CH_3, R'= OCH_3
3h: R= CH_3, R'= Br
3i : R= OCH_3, R'=H
3j: R= OCH_3, R'= CH_3
3k: R= OCH_3, R'= OCH_3
3l: R= OCH_3, R'= Br
3m: R= Cl, R'=H
3n: R= Cl, R'= CH_3
3o: R= Cl, R'= OCH_3
3p: R= Cl, R'= Br

Scheme 1.

Table 1
^{13}C NMR spectral data of compounds10a-phenylbenzo[*b*]indeno[1,2-*e*][1,4]thiazin-11(10a*H*)-ones (**3a**–**3p**).

Comp.	C_1	C_2	C_3	C_4	C_{4a}	C_{4b}	C_{5a}	C_6	C_7	C_8	C_9	C_{9a}	C_{10a}	$C_{1'}$	$C_{2'}$	$C_{3',5'}$	$C_{4'}$	$C_{6'}$	C_{11a}	C_{11}	R = H/CH_3/OCH_3/Cl	R′ = H/CH_3/OCH_3/Br
3a	125.45	129.62	129.84	126.80	133.88	165.21	134.68	119.99	121.85	125.40	123.02	119.39	118.34	129.47	128.35	127.70	130.82	128.26	131.46	182.34	–	–
3b	125.73	130.47	130.78	127.10	134.61	165.20	135.63	123.13	126.75	135.30	121.86	119.64	118.35	129.84	129.52	128.43	130.08	128.23	131.37	184.22	–	20.54
3c	121.85	129.56	129.65	122.87	131.26	164.88	134.61	121.27	112.52	156.52	117.64	120.61	110.68	128.48	128.29	126.87	129.89	127.23	130.71	184.40	–	55.55
3d	122.34	130.48	130.79	127.70	134.19	165.20	135.61	120.64	123.14	128.17	121.97	117.95	110.23	130.08	129.76	128.57	131.75	129.47	132.97	184.14	–	–
3e	126.44	129.49	130.75	127.88	132.56	164.67	133.60	119.74	121.90	126.36	123.25	118.96	118.32	130.88	128.77	128.28	140.38	129.28	131.48	183.82	21.51	–
3f	126.32	130.62	130.95	127.62	133.15	162.23	136.31	123.96	126.12	139.52	121.46	118.38	117.95	131.72	130.10	128.23	140.23	129.65	132.23	183.75	21.58	20.58
3g	122.81	128.43	129.35	126.74	131.20	164.85	131.58	121.92	112.47	156.48	120.58	121.39	117.87	130.32	128.35	127.23	139.98	128.19	130.77	183.90	21.57	55.53
3h	126.60	130.84	131.15	127.65	132.94	165.19	136.43	122.03	126.85	128.10	123.07	117.89	118.96	131.69	130.38	128.46	140.23	129.26	131.96	183.78	21.58	–
3i	126.34	129.26	130.82	126.56	132.62	164.70	133.61	121.96	123.25	126.25	124.15	121.81	119.86	131.11	128.27	115.72	160.94	127.87	131.48	184.25	55.58	–
3j	123.08	128.28	128.42	125.68	131.30	165.07	135.24	121.90	122.92	134.38	119.85	119.51	119.24	130.00	128.12	115.01	160.70	126.80	130.85	184.67	55.43	20.65
3k	126.02	130.42	131.15	127.11	134.71	164.28	136.60	122.96	112.48	156.60	115.01	115.18	113.01	130.61	130.03	115.85	159.60	129.42	132.85	184.92	55.60	55.48
3l	126.43	130.01	130.48	127.73	133.61	165.81	136.88	121.96	125.85	129.72	123.01	120.02	113.45	130.95	128.56	114.98	159.53	128.01	131.20	184.70	55.55	–
3m	126.36	129.49	130.25	126.43	133.16	164.60	134.09	120.43	122.56	126.01	124.13	119.43	118.01	130.70	129.28	127.87	133.59	128.28	131.48	184.35	–	–
3n	125.74	129.64	129.84	126.75	134.75	165.09	136.27	122.95	128.24	140.23	121.86	119.65	113.72	130.78	129.52	128.37	135.32	128.43	131.35	184.42	–	20.56
3o	121.71	130.03	130.52	123.02	133.07	164.81	136.81	120.93	112.61	156.58	116.12	120.62	110.70	131.11	128.55	127.11	136.00	127.19	131.41	184.72	–	55.55
3p	123.30	130.60	131.01	127.08	133.02	165.21	140.10	120.65	126.15	128.82	121.83	118.05	116.07	131.90	130.14	127.72	136.23	128.24	132.66	184.57	–	–

to C_{11}-carbonyl group [45] and the signals in the aromatic regions at *δ* 121.71–126.60, *δ* 128.28–130.84, *δ* 128.42–131.15, *δ* 122.87–127.88, *δ* 131.20–134.75 and *δ* 130.71–132.97 are in accord with the observed trends for carbon atoms C_1, C_2, C_3, C_4, C_{4a} and C_{11a} of indanone moiety [46] respectively. The signals in the regions *δ* 162.23–165.81, *δ* 131.58–140.10, *δ* 119.74–123.96, *δ* 112.47–128.24, *δ* 125.40–156.60, *δ* 115.01–124.15, *δ* 115.18–121.81 and *δ* 110.23–119.86 are assigned to C_{4b}, C_{5a}, C_6, C_7, C_8, C_9, C_{9a} and C_{10a} respectively which are in obeisance with the values reported in the literature [47–49]. With the variation of R′ the change in chemical shift values due to C_8 signal was observed [50]. The signals due to remaining aromatic and aliphatic carbons were observed in the expected regions (Table 1). Further, the mass spectral data and analytical data of **3a**–**3p** are in good agreement with their molecular formula.

2.2. Biological section

2.2.1. Antibacterial activity

All the synthesized compounds were screened for their *in vitro* antibacterial activity against two Gram-positive bacteria *viz*. *Bacillus subtilis* (MTCC 441) and *Staphylococcus aureus* (MTCC 7443), Gram-negative bacteria *viz*. *Escherichia coli* (MTCC 42) and *Pseudomonas aeruginosa* (MTCC 7952). Minimum inhibitory concentrations (MIC) were determined using serial dilution technique [51]. While carrying out antibacterial activity penicillin and streptomycin were used as reference compounds and MIC were determined in term of μmol/mL (Table 2, Fig. 1).

It is revealed from the data presented in Table 2 and Fig. 1 that the compounds **3b**, **3d**, **3k** and **3m** exhibited very promising antibacterial activity against Gram positive (*B. subtilis* and *S. aureus*) and Gram negative (*E. coli* and *P. aeruginosa*) bacteria. The compound **3m** was most effective against *E. coli*. Compound **3d** showed very high activity against *P. aeruginosa*. The compounds **3k** (MIC, 0.0040 μmol/mL) and **3b** (MIC, 0.0045 μmol/mL) exhibited notable activity, almost comparable to penicillin (MIC, 0.0046 μmol/mL) for *B. subtilis* and *S. aureus* respectively. However, **3i** exhibited negligible activity against *B. Subtilis* and *P. aeruginosa*,

Table 2
In vitro antibacterial activity of 1,4-benzothiazines (**3a**–**3p**).

Minimum inhibitory concentration (MIC)[a]				
Compounds	Gram-positive bacteria		Gram-negative bacteria	
	B. subtilis[b]	*S. aureus*[c]	*E. coli*[d]	*P. aeruginosa*[e]
3a	0.0764	0.1528	0.0382	0.0382
3b	0.1465	0.0045	–	0.0733
3c	0.0700	0.1400	–	0.0350
3d	0.0617	0.1234	0.0617	0.0154
3e	0.0732	0.2931	–	0.0732
3f	0.1408	–	0.0352	0.0704
3g	0.0673	0.1347	0.0042	0.0336
3h	0.0298	0.1193	0.0594	0.0594
3i	–	0.1400	0.0700	–
3j	0.0336	0.0673	0.0673	0.0673
3k	0.0040	0.0161	0.0161	–
3l	0.0071	0.0071	0.0143	0.0574
3m	0.0346	0.1384	0.0043	–
3n	0.0665	–	0.0666	0.0666
3o	0.0319	0.0159	0.0639	0.0639
3p	0.0284	0.0071	0.0569	0.0570
Penicillin	0.0046	0.0046	0.0374	0.0187
Streptomycin	0.0107	0.0107	0.0053	0.0026

[a] Unit: μmol/mL.
[b] *Bacillus subtilis* (MTCC 441).
[c] *Staphylococcus aureus* (MTCC 7443).
[d] *Escherichia coli* (MTCC 42).
[e] *Pseudomonas aeruginosa* (MTCC 7952).

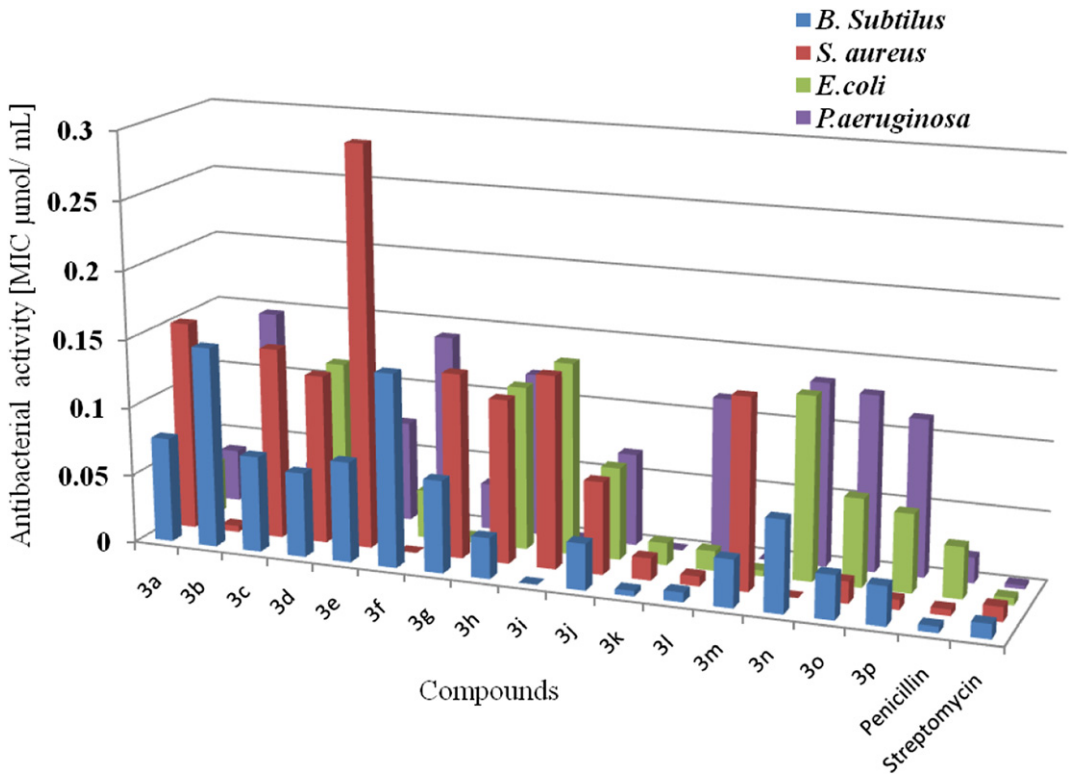

Fig. 1. Graphical representation of *in vitro* antibacterial activity of 10a-phenylbenzo[*b*]indeno[1,2-*e*][1,4]thiazin-11(10a*H*)-ones (**3a**–**3p**).

3f and **3n** against *S. aureus*, **3b**, **3c** and **3e** against *E. coli* and **3k** and **3m** against *P. aeruginosa.*

Percent change in antibacterial activity of different derivatives **3b**–**3p** over parent compound 10a-phenylbenzo[*b*]indeno[1,2-*e*][1,4]thiazin-11(10a*H*)-one (**3a**) were calculated using the following formula.

Percent change in antibacterial activity = (P − D)/P × 100

Where P and D are Minimum inhibitory concentrations (MIC) in µmol/mL for the parent compound and derivative respectively (Table 3, Fig. 2).

A perusal of data from Table 3 and Fig. 2 reveals that derivatives **3h**, **3j**, **3k**, **3l**, **3m**, **3o** and **3p** exhibited high activity against *B. subtilis*, **3b**, **3j**, **3k**, **3l**, **3o** and **3p** against *S. aureus*, **3j**, **3k**, **3l** and **3m** against *E. coli* and **3d** against *P. aeruginosa* compared to the parent compound **3a**. The derivatives **3c**, **3d**, **3e**, **3g** and **3n** were moderately active against *B. subtilis*, **3c**, **3d**, **3g**, **3h**, **3i** and **3m** against *S. aureus*, **3f** and **3g** against *E. coli*, and **3c** and **3g** against *P. aeruginosa* as compared to the parent compound **3a**. Further, the derivatives **3b** and **3f** exhibited lower percent change in antibacterial activity against *B. subtilis*, **3e** against *S. aureus*, **3d**, **3h**, **3i**, **3n**, **3o** and **3p** against *E. coli* and **3b**, **3e**, **3f**, **3h**, **3j**, **3l**, **3n**, **3o** and **3p** against *P. aeruginosa* as compared to the parent compound **3a**. However, some of the derivatives did not show any percent change in antibacterial activity over parent compound **3a**, amongst them were **3i** against *B. subtilis*, **3f** against *S. aureus*, **3b**, **3c** and **3e** against *E. coli* and **3i**, **3k** and **3m** against *P. aeruginosa*. Also, from the above data, it is inferred that out of derivatives **3b**–**3p**, the benzothiazines **3j**, **3k** and **3l**, where R = OCH_3 and R′ = CH_3, OCH_3 and Br respectively are more effective than the parent compound **3a** for the respective bacteria *B. subtilis*, *S. aureus* and *E. coli* and resulted in the pattern CH_3 > Br > OCH_3 towards their antibacterial activity and lower activity is shown by most of the derivatives against *P. aeruginosa* compared to the parent compound **3a**. However, no general rule toward structure–activity relationship has been established for their antibacterial activity.

2.2.2. Antifungal activity

All the synthesized compounds were screened for their *in vitro* antifungal activity against two fungi *viz. Aspergillus fumigates* (MTCC 2550) and *Candida albicans* (MTCC 183). Minimum

Table 3
Percent change[a] in antibacterial activity of 1,4-benzothiazines (**3b**–**3p**) over parent compound **3a**.

Compounds	Gram-positive bacteria		Gram-negative bacteria	
	B. subtilis[b]	*S. aureus*[c]	*E. coli*[d]	*P. aeruginosa*[e]
3a	–	–	–	–
3b	−91.75	97.05	–	−91.88
3c	8.37	8.37	–	8.38
3d	1.92	19.24	−61.51	59.68
3e	4.18	−91.81	–	−91.62
3f	−84.29	–	7.85	−84.29
3g	11.91	11.84	8.90	12.04
3h	60.99	21.92	−55.49	−55.49
3i	–	8.37	−83.24	–
3j	56.02	55.95	76.17	−76.17
3k	94.76	89.46	57.85	–
3l	90.70	95.35	62.56	−50.26
3m	54.71	9.42	88.74	–
3n	12.95	–	−74.34	−74.34
3o	58.24	89.59	−67.25	−67.27
3p	62.82	95.35	−49.95	−49.21

[a] Percent change in antibacterial activity = (P − D)/P × 100. Where P and D are Minimum inhibitory concentrations (MIC) in µmol/mL for the parent compound and derivative respectively.
[b] *Bacillus subtilis* (MTCC 441).
[c] *Staphylococcus aureus* (MTCC 7443).
[d] *Escherichia coli* (MTCC 42).
[e] *Pseudomonas aeruginosa* (MTCC 7952).

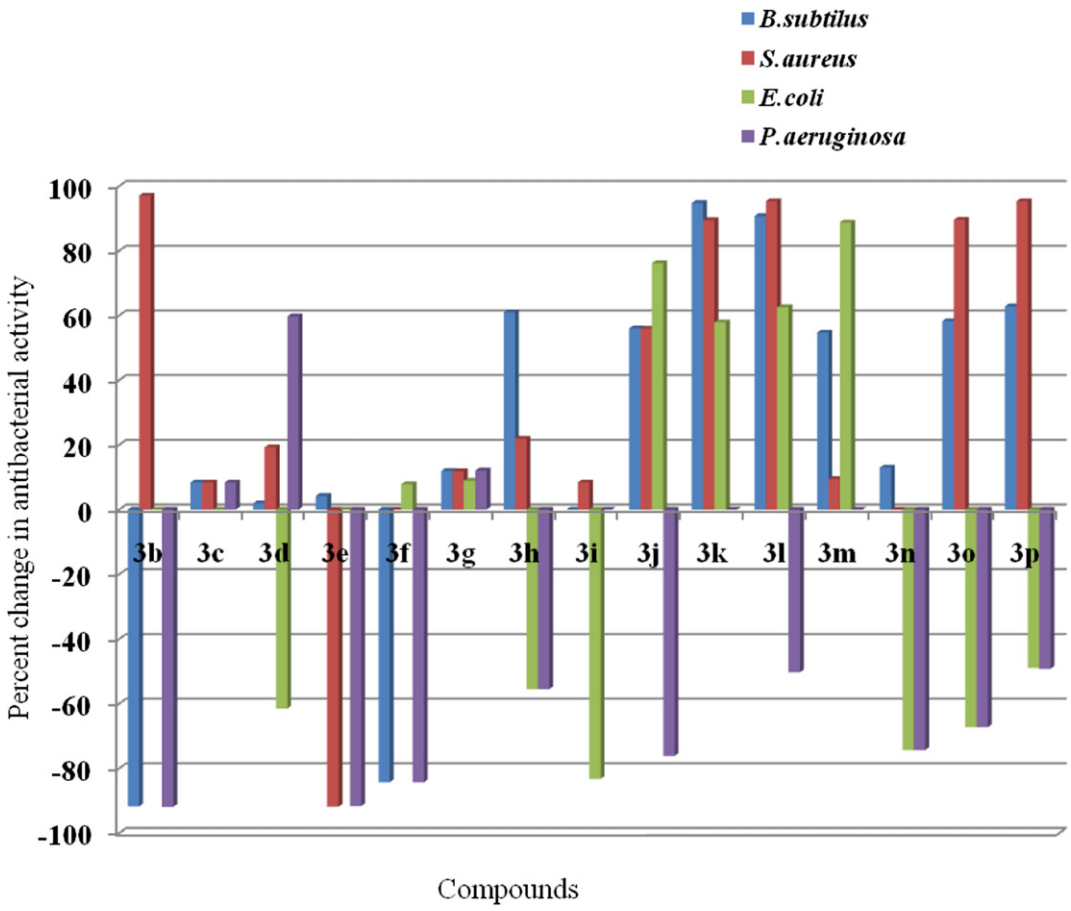

Fig. 2. Percent change in antibacterial activity of 1,4-benzothiazines (**3b**–**3p**) over parent compound **3a**.

inhibitory concentrations (MIC) were determined using Serial dilution technique [51]. While carrying out antifungal activity fluconazole was used as reference compound and MIC were determined in term of μmol/mL (Table 4, Fig. 3).

The data presented in Table 4 and Fig. 3 reveals that the compounds **3c**, **3e**, **3i** and **3m** were found to be inactive against fungi *A. fumigates* and *C. albicans*. The compounds **3e**, **3i** and **3m** have a common structural feature i.e. they have no substituent on C_8. The antifungal activities of other compounds were moderate, however, compound **3l** is most effective against *A. fumigates* and **3g** and **3l** exhibit high activity against *C. albicans*. The percent change in antifungal activity of different derivatives **3b**–**3p** over parent compound 10a-phenylbenzo[*b*]indeno[1,2-*e*][1,4]thiazin-11(10a*H*)-one (**3a**) was calculated using the same formula as employed for antibacterial activity (Table 5, Fig. 4).

Table 4
In vitro antifungal activity of 1,4-benzothiazines (**3a**–**3p**).

Compounds	Minimum inhibitory concentration (MIC)[a]	
	A. fumigates[b]	*C. albicans*[c]
3a	0.0764	0.0764
3b	0.0732	0.0366
3c	–	–
3d	0.0308	0.0308
3e	–	–
3f	0.1408	0.0704
3g	0.0673	0.0168
3h	0.1193	0.1193
3i	–	–
3j	0.1347	0.0336
3k	0.0645	0.0645
3l	0.0143	0.0143
3m	–	–
3n	0.1333	0.0666
3o	0.0319	0.0319
3p	0.0284	0.0284
Fluconazole	0.0101	0.0101

[a] Unit: μmol/mL.
[b] *Aspergillus fumigates* (MTCC 2550).
[c] *Candida albicans* (MTCC 183).

It is inferred from the data presented in Table 5 and Fig. 4 that the derivatives **3b**, **3d**, **3f**, **3g**, **3j**, **3l**, **3o** and **3p** exhibited high activity against *C. albicans* and the derivatives **3d**, **3l**, **3o** and **3p** against *A. fumigates* as compared to parent compound **3a**. The derivatives **3k** and **3n** exhibited nearly same activity against *C. albicans*, **3g** and **3k** against *A. fumigates* as shown by parent compound **3a**. The derivative **3h** showed lower percent change in activity against *C. albicans* and the derivatives **3f**, **3h**, **3j** and **3n** against *A. fumigates* as compared to parent compound **3a**, while the derivatives **3c**, **3e**, **3i** and **3m** did not show any significant change in their antifungal activity against *C. albicans* and *A. fumigates* over parent compound **3a**.

2.3. QSAR studies

In order to understand the experimental antimicrobial data on a theoretical basis, we established a quantitative structure–activity relationship (QSAR) between the *in vitro* antimicrobial activity of synthesized 10a-phenylbenzo[*b*]indeno[1,2-*e*][1,4]thiazin-11(10a*H*)-ones (**3a**–**3p**) and descriptors coding for lipophilic, electronic, steric

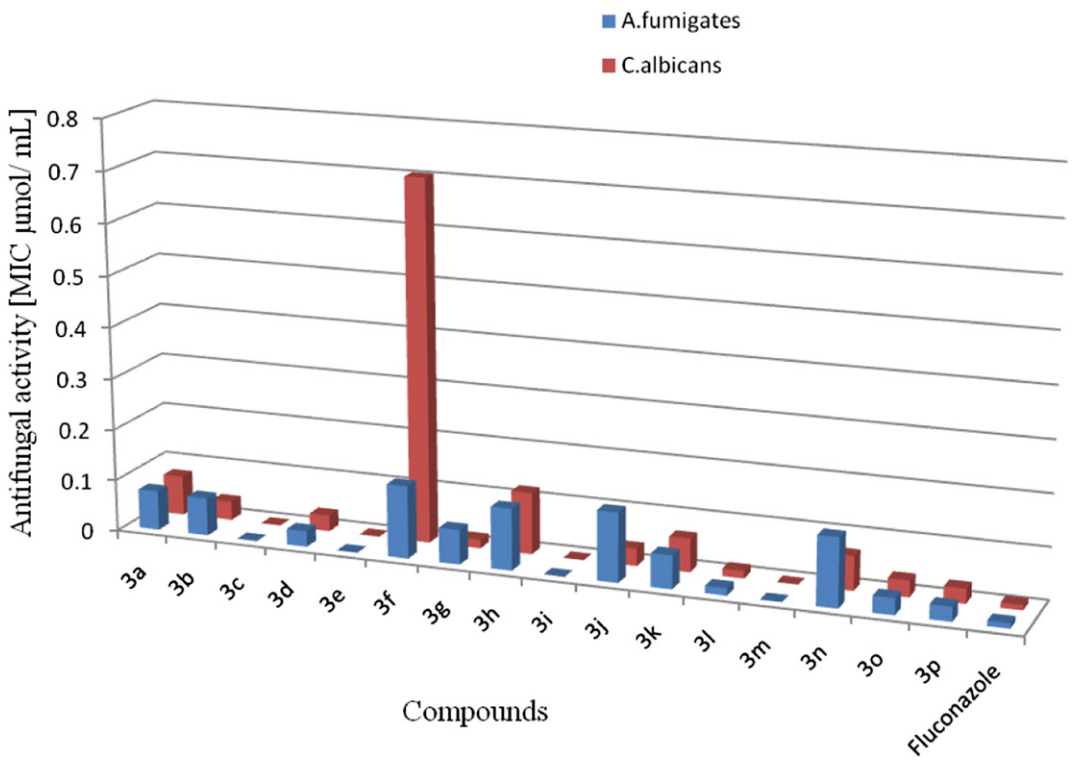

Fig. 3. Graphical representation of *in vitro* antifungal activity of 10a-phenylbenzo[*b*]indeno[1,2-*e*][1,4]thiazin-11(10a*H*)-ones (**3a**–**3p**).

and topological properties of the molecules under consideration using the linear free energy relationship model (LFER) described by Hansch and Fujita [52]. Biological activity data determined as MIC values were first transformed into pMIC values and used as dependent variables in a QSAR study and are presented in Table 6. The different molecular descriptors (independent variables) like log of octanol–water partition coefficient (log *P*), molar refractivity (MR), Kier's molecular connectivity ($^{n}\chi$, $^{n}\chi^{v}$) and shape (κ_n, $\kappa\alpha_n$) topological indices, Randic topological index (R), Balaban topological index (J), Wiener topological index (W), Total energy (Te), energies of highest occupied molecular orbital (HOMO) and lowest unoccupied molecular orbital (LUMO), dipole moment (μ), electronic energy (Ele.E), nuclear energy (Nu.E) and molecular surface area (SA) calculated for the synthesized 10a-phenylbenzo[*b*]indeno[1,2-*e*][1,4]thiazin-11(10a*H*)-ones (**3a**–**3p**) are used as independent variables and the values of selected descriptors used in the regression analysis are presented in Table 7 [53–58].

In the present study, a data set of sixteen 10a-phenylbenzo[*b*]indeno[1,2-*e*][1,4]thiazin-11(10a*H*)-ones (**3a**–**3p**) was subjected to linear free energy regression analysis for model generation. Preliminary analysis was carried out in terms of correlation analysis. A correlation matrix constructed for antibacterial activity against *S. aureus* is presented in Table 8. The correlations of different molecular descriptor with antimicrobial activity are presented in Table 9. In general, high collinearity ($r > 0.8$) was observed between most of the parameters. The high interrelationship was observed between $\kappa\alpha_1$ and $\kappa\alpha_3$ ($r = 0.993$) and low interrelationship was observed between $\kappa\alpha_2$ and LUMO ($r = 0.026$).

In the present study, different outliers are identified against different microorganisms, and the models have been developed after removal of the outliers (compound numbers in brackets) *B. subtilis* (**3a**, **3f**, **3m**), *S. aureus* (**3b**, **3g**, **3h**), *E. coli* (**3g**, **3k**, **3l**, **3m**), *P. aeruginosa* (**3b**, **3d**, **3e**, **3g**), *A. fumigates* (**3h**, **3n**) and *C. albicans* (**3g**, **3h**, **3k**). In multivariate statistics, it is common to define three types of outliers [59].

1. *X*/*Y* relation outliers are substances for which the relationship between the descriptors (*X* variables) and the dependent variables (*Y* variables) is not the same as in the (rest of the) training data.
2. *X* outliers are substances whose molecular descriptors do not lie in the same range as the (rest of the) training data.
3. *Y* outliers are only defined for training or test samples. They are substances for which the reference value of response is invalid.

As there was no difference in the activity (Table 6) as well as the molecular descriptor range (Table 7) of these outliers when

Table 5
Percent change[a] in antifungal activity of 1,4-benzothiazines (**3b**–**3p**) over parent compound **3a**.

Compounds	*A. fumigates*[b]	*C. albicans*[c]
3a	–	–
3b	4.18	52.09
3c	–	–
3d	59.68	59.68
3e	–	–
3f	−84.29	78.53
3g	11.91	78.01
3h	−56.15	−56.15
3i	–	–
3j	−76.3	56.02
3k	15.57	15.57
3l	81.28	81.28
3m	–	–
3n	−74.47	12.82
3o	58.24	58.24
3p	62.82	62.82

[a] Percent change in antifungal activity = (P − D)/P × 100. Where P and D are Minimum inhibitory concentrations (MIC) in µmol/mL for the parent compound and derivative respectively.
[b] *Aspergillus fumigates* (MTCC 2550).
[c] *Candida albicans* (MTCC 183).

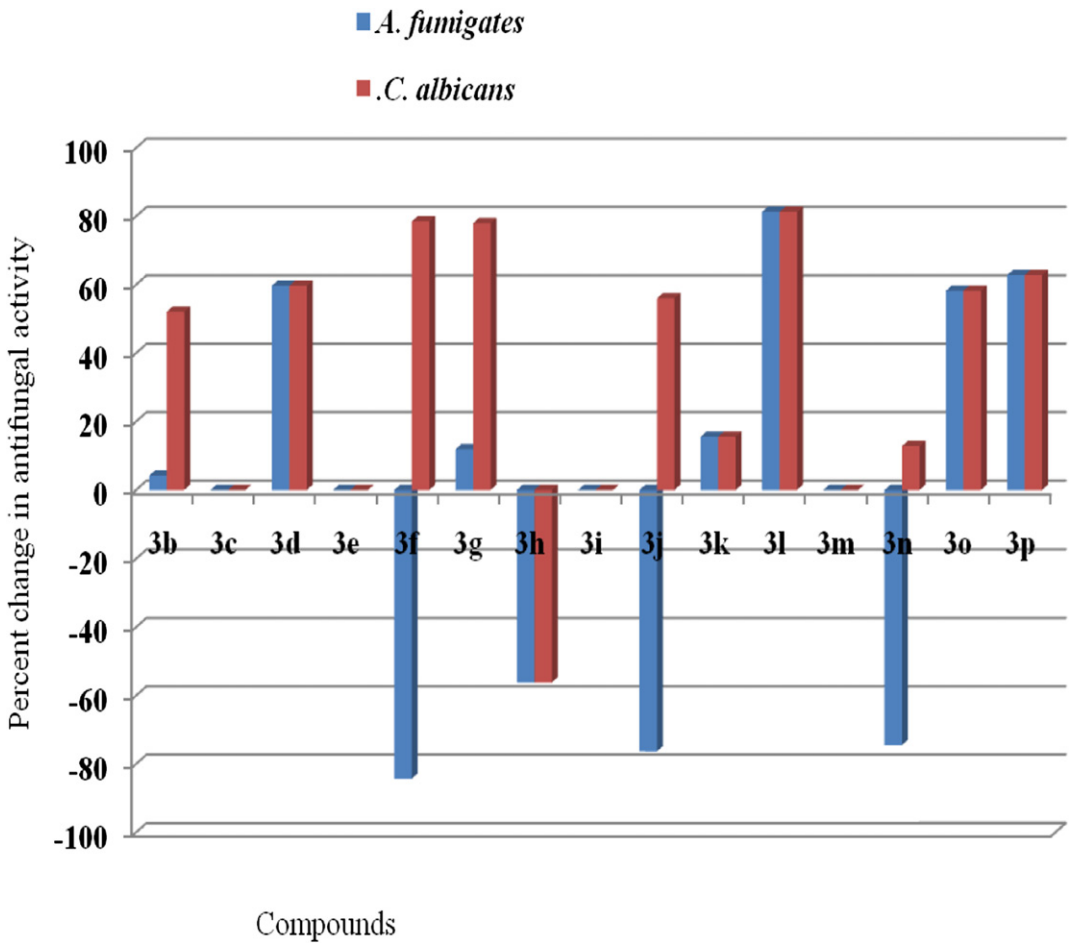

Fig. 4. Percent change in antifungal activity of 1,4-benzothiazines (**3b**–**3p**) over parent compound **3a**.

compared to other 10a-phenylbenzo[*b*]indeno[1,2-*e*][1,4]thiazin-11(10a*H*)-ones indicated the fact that these outliers belong to the category of Y outliers (Substances for which the reference value of response is invalid).

Correlation matrix (Table 8) indicated the importance of the topological parameter, Kiers second order alpha shape index ($\kappa\alpha_2$) in describing antibacterial activity of synthesized 10a-phenylbenzo[*b*]indeno[1,2-*e*][1,4]thiazin-11(10a*H*)-ones (**3a**–**3p**) against *B. subtilis* (Eq. (1)).

QSAR model for antibacterial activity against B. subtilis

$$\text{pMICbs} = 0.987\kappa\alpha_2 - 4.434 \quad (1)$$

$$n = 12 \quad r = 0.849 \quad q^2 = 0.566 \quad s = 0.247 \quad F = 25.86$$

Here and thereafter, n – number of data points, r – correlation coefficient, q^2 – cross-validated r^2 obtained by leave one out method, s – standard error of the estimate and F – Fischer statistics.

As the coefficient of $\kappa\alpha_2$ in Eq. (1) is positive, therefore the antibacterial activity against *B. subtilis* will increase with increase in value of $\kappa\alpha_2$. This is clearly evident from Table 7 that compound **3k** having high $\kappa\alpha_2$ value of 6.63 have higher pMICbs value (pMICbs = 2.40, Table 6) than the other compounds. Similarly, compound **3b** having low $\kappa\alpha_2$ value of 5.37 (Table 7), has minimum antibacterial activity against *B. subtilis* (pMICbs = 0.83, Table 6).

The QSAR model expressed by Eq. (1) was cross validated by its appreciable q^2 values ($q^2 = 0.566$) obtained by leave one out (LOO) method. The value of q^2 greater than 0.5 is the basic requirement for qualifying a QSAR model to be valid one [60]. The comparison of observed and predicted antimicrobial activities is presented in Table 10. It can be seen from the results that the observed and predicted antimicrobial activities lie close to each other as evidenced by their low residual values. The plot of predicted pMICbs against observed pMICbs (Fig. 5) also favours the model expressed

Table 6
In vitro antimicrobial activity of compounds 10a-phenylbenzo[*b*]indeno[1,2-*e*][1,4]thiazin-11(10a*H*)-ones (**3a**–**3p**).

Comp.	pMICbs	pMICsa	pMICec	pMICpa	pMICaf	pMICca
3a	1.12	0.82	1.42	1.42	1.12	1.12
3b	0.83	2.35	–	1.13	1.14	1.44
3c	1.15	0.85	–	1.46	–	–
3d	1.21	0.91	1.21	1.81	1.51	1.51
3e	1.14	0.53	–	1.14	–	–
3f	0.85	–	1.45	1.15	0.85	1.15
3g	1.17	0.87	2.38	1.47	1.17	1.77
3h	1.53	0.92	1.23	1.23	0.92	0.92
3i	–	0.85	1.15	–	–	–
3j	1.47	1.17	1.17	1.17	0.87	1.47
3k	2.40	1.79	1.79	–	1.19	1.19
3l	2.15	2.15	1.84	1.24	1.84	1.84
3m	1.46	0.86	2.37	–	–	–
3n	1.18	–	1.18	1.18	0.88	1.18
3o	1.50	1.80	1.19	1.19	1.50	1.50
3p	1.55	2.15	1.24	1.24	1.55	1.55
S.D.[a]	0.43	0.62	0.45	0.20	0.32	0.28

[a] S.D. Standard deviation.

Table 7
Values of selected parameters used in regression analysis.

Comp.	log *P*	MR	$^{3}\chi$	$\kappa\alpha_2$	Te	LUMO	HOMO	μ
3a	4.35	97.86	1.48	5.12	−3586.64	−1.05	−8.38	2.49
3b	4.82	102.90	1.77	5.37	−3742.52	−1.03	−8.35	2.42
3c	4.10	104.32	1.69	5.87	−4062.50	−1.00	−8.38	3.67
3d	5.15	105.48	1.77	5.62	−3926.23	−1.25	−8.55	3.20
3e	4.82	102.90	1.77	5.37	−3742.52	−1.03	−8.36	2.75
3f	5.29	107.94	2.06	5.62	−3898.39	−1.01	−8.32	2.69
3g	4.57	109.36	1.98	6.12	−4218.37	−0.98	−8.35	3.83
3h	4.10	104.32	1.69	5.87	−4062.51	−1.04	−8.35	3.64
3i	5.61	110.52	2.06	5.87	−4082.10	−1.23	−8.52	3.43
3j	4.57	109.36	1.98	6.12	−4218.39	−1.02	−8.32	3.57
3k	3.85	110.78	1.89	6.63	−4538.37	−0.99	−8.35	4.86
3l	4.89	111.94	1.98	6.37	−4402.10	−1.24	−8.51	4.22
3m	5.34	107.70	2.06	5.77	−4102.62	−1.11	−8.44	2.28
3n	4.87	102.66	1.77	5.52	−3946.75	−1.13	−8.48	2.38
3o	4.62	109.12	1.98	6.27	−4422.61	−1.08	−8.47	3.62
3p	5.66	110.28	2.06	6.02	−4286.33	−1.33	−8.63	3.12

by Eq. (1). Further, the plot of observed pMICbs *vs* residual pMICbs (Fig. 6) indicated that there was no systemic error in model development as the propagation of residuals was observed on both positive and negative sides [61].

According to Kier, the shape of a molecule may be partitioned into attributes, each describable by the count of bonds of various path lengths. The basis for devising a relative index of shape is given by the relationship of the number of path of length *l* in the molecule *i*, $^{l}P_i$, to some reference values based on molecules with a given number of atoms, *n*, in which the values of ^{l}P are maximum and minimum, $^{l}P_{max}$ and $^{l}P_{min}$ [62].

The modified kappa shape indices are given by:

$$\kappa\alpha_1 = (n+\alpha)(n+\alpha-1)^2/(^1P_i+\alpha)^2$$

$$\kappa\alpha_2 = (n+\alpha-1)(n+\alpha-2)^2/(^2P_i+\alpha)^2$$

$$\kappa\alpha_3 = (n+\alpha-1)(n+\alpha-3)^2/(^3P_i+\alpha)^2 \text{ n is odd}$$

$$\kappa\alpha_3 = (n+\alpha-3)(n+\alpha-2)2/(^3P_i+\alpha)^2 \text{ n is even}$$

In case of *S. aureus*, the developed QSAR model (Eq. (2)) indicated the predominance of valence zero order molecular connectivity index ($^{0}\chi^{v}$) in describing the antibacterial activity.

QSAR model for antibacterial activity against S. aureus

$$\text{pMICsa} = 0.525\ ^{0}\chi^{v} - 6.689 \quad (2)$$

Table 9
Correlation of antimicrobial activity of compounds10a-phenylbenzo[*b*]indeno[1,2-*e*][1,4]thiazin-11(10a*H*)-ones (**3a**–**3p**) with studied molecular descriptors.

	pMICbs	pMICsa	pMICec	pMICpa	pMICaf	pMICca
log *P*	−0.248	0.283	0.093	−0.619	0.266	0.042
MR	0.771	0.843	−0.431	−0.726	0.315	0.610
$^{0}\chi$	0.757	0.702	−0.519	−0.653	0.094	0.512
$^{0}\chi^{v}$	0.752	0.883	−0.478	−0.630	0.507	0.703
$^{1}\chi$	0.752	0.641	−0.572	−0.504	0.087	0.555
$^{1}\chi^{v}$	0.669	0.877	−0.426	−0.627	0.561	0.695
$^{2}\chi$	0.702	0.776	−0.406	−0.805	0.102	0.428
$^{2}\chi^{v}$	0.379	0.789	−0.266	−0.658	0.574	0.584
κ_1	0.758	0.679	−0.542	−0.599	0.091	0.530
κ_2	0.736	0.577	−0.598	−0.341	0.079	0.585
κ_3	0.761	0.680	−0.539	−0.599	0.088	0.524
$\kappa\alpha_1$	0.821	0.804	−0.593	−0.620	0.280	0.625
$\kappa\alpha_2$	0.849	0.780	−0.697	−0.442	0.334	0.714
$\kappa\alpha_3$	0.829	0.843	−0.593	−0.615	0.346	0.645
R	0.752	0.641	−0.572	−0.504	0.087	0.555
J	−0.749	−0.451	0.608	0.295	−0.084	−0.589
W	0.772	0.666	−0.551	−0.582	0.084	0.539
Te	−0.817	−0.835	0.690	0.470	−0.408	−0.671
El. E	−0.763	−0.672	0.557	0.578	−0.094	−0.538
Nu. E	0.746	0.645	−0.528	−0.584	0.050	0.510
LUMO	−0.191	−0.494	0.242	0.207	−0.780	−0.600
HOMO	−0.184	−0.522	0.260	0.071	−0.838	−0.535
μ	0.809	0.572	−0.584	0.042	0.326	0.843

$$n = 11 \quad r = 0.883 \quad q^2 = 0.559 \quad s = 0.293 \quad F = 31.70$$

The coefficient of $^{0}\chi^{v}$ is positive in Eq. (2), which indicates that the antibacterial activity will increase with the increase in $^{0}\chi^{v}$ of the synthesized compounds, which can be clearly seen from the results of antibacterial activity against *S. aureus* (Table 6) and values of $^{0}\chi^{v}$ presented in Table 7.

The topological index, $^{0}\chi$, signifies the degree of branching, connectivity of atoms and the unsaturation in the molecule which accounts for variation in the activity [63]. In order to account for the variation in size contribution to shape from different atoms the radius of atom X relative to the covalent radius of a carbon sp^3 hybrid atom is considered. The specific correction in computing $^{1}\kappa$ is made by modifying the count of atoms, *n*, with a modifier, *a*, calculated as:

$$\alpha_X = \left(r_X/r_{csp^3}\right) - 1$$

Where α represents a decrement or increment of *n* for a non carbon sp^3 element X.

For antibacterial activity against *E. coli*, the developed QSAR model (Eq. (3)) depicted the importance of Kier's alpha shape topological index ($\kappa\alpha_2$). In this case, a negative correlation was observed between $\kappa\alpha_2$ and antibacterial activity against *E. coli*.

Table 8
Correlation matrix of synthesized compounds10a-phenylbenzo[*b*]indeno[1,2-*e*][1,4]thiazin-11(10a*H*)-ones (**3a**–**3p**) against *S. aureus*.

	pMICbs	log *P*	MR	$^{0}\chi$	$^{0}\chi^{v}$	$^{3}\chi$	$\kappa\alpha_1$	$\kappa\alpha_2$	$\kappa\alpha_3$	Te	LUMO	HOMO	μ
pMICbs	1.000	−0.248	0.771	0.757	0.752	0.355	0.821	0.849	0.829	−0.817	−0.191	−0.184	0.809
log *P*		1.000	0.118	−0.444	0.261	0.517	−0.268	−0.398	−0.171	0.273	−0.805	−0.729	−0.589
MR			1.000	0.814	0.969	0.804	0.911	0.846	0.940	−0.869	−0.356	−0.362	0.622
$^{0}\chi$				1.000	0.679	0.507	0.968	0.961	0.934	−0.930	0.214	0.153	0.792
$^{0}\chi^{v}$					1.000	0.773	0.830	0.771	0.883	−0.817	−0.562	−0.574	0.559
$^{3}\chi$						1.000	0.603	0.453	0.650	−0.548	−0.418	−0.404	0.062
$\kappa\alpha_1$							1.000	0.984	0.993	−0.983	−0.032	−0.098	0.783
$\kappa\alpha_2$								1.000	0.970	−0.981	0.026	−0.053	0.864
$\kappa\alpha_3$									1.000	−0.984	−0.143	−0.209	0.752
Te										1.000	0.082	0.182	−0.768
LUMO											1.000	0.958	0.142
HOMO												1.000	0.085
μ													1.000

Table 10
Comparison of observed and predicted antibacterial and antifungal activity obtained by ot-QSAR model.

Comp.	pMICbs			pMICsa			pMICec			pMICpa			pMICaf			pMICca		
	Obs	Pre	Res	Obs	Pre	Res	Obs	Pre	Res	Obs	Pre	Res	Obs	Pre	Res	Obs	Pre	Res
3a	1.12	0.62	0.50	0.82	0.30	0.52	1.42	1.41	0.01	1.42	1.47	−0.05	1.12	1.18	−0.06	1.12	1.24	−0.12
3b	0.83	0.87	−0.03	2.35	0.78	1.56	–	**1.35**	–	1.13	1.33	−0.19	1.14	1.09	0.05	1.44	1.22	0.21
3c	1.15	1.36	−0.20	0.85	1.00	−0.14	–	**1.24**	–	1.46	1.37	0.09	–	**1.17**	–	–	**1.59**	–
3d	1.21	1.11	0.10	0.91	1.31	−0.40	1.21	1.29	−0.08	1.81	1.33	0.48	1.51	1.57	−0.06	1.51	1.45	0.06
3e	1.14	0.87	0.27	0.53	0.78	−0.25	–	**1.35**	–	1.14	1.33	−0.19	–	**1.11**	–	–	**1.32**	–
3f	0.85	1.12	−0.26	–	**1.27**	–	1.45	1.29	0.16	1.15	1.19	−0.04	0.85	1.02	−0.17	1.15	1.30	−0.15
3g	1.17	1.60	−0.43	0.87	1.48	−0.61	2.38	1.18	1.20	1.47	1.23	0.24	1.17	1.10	0.07	1.77	1.64	0.13
3h	1.53	1.36	0.17	0.92	1.00	−0.07	1.23	1.24	−0.01	1.23	1.37	−0.14	0.92	1.11	−0.19	0.92	1.59	−0.66
3i	–	**1.36**	–	0.85	1.79	−0.94	1.15	1.24	−0.08	–	**1.19**	–	–	**1.50**	–	–	**1.52**	–
3j	1.47	1.60	−0.13	1.17	1.48	−0.31	1.17	1.18	−0.01	1.17	1.23	−0.06	0.87	1.02	−0.15	1.47	1.56	−0.09
3k	2.40	2.11	0.29	1.79	1.70	0.10	1.79	1.06	0.73	–	**1.27**	–	1.19	1.10	0.09	1.19	1.95	−0.76
3l	2.15	1.85	0.30	2.15	2.01	0.14	1.84	1.12	0.72	1.24	1.23	0.01	1.84	1.49	0.36	1.84	1.76	0.09
3m	1.46	1.26	0.20	0.86	1.37	−0.51	2.37	1.26	1.11	–	**1.19**	–	–	**1.31**	–	–	**1.18**	–
3n	1.18	1.01	0.16	–	**0.89**	–	1.18	1.32	−0.14	1.18	1.33	−0.15	0.88	1.40	−0.53	1.18	1.21	−0.03
3o	1.50	1.75	−0.26	1.80	1.58	0.21	1.19	1.15	0.05	1.19	1.23	−0.04	1.50	1.38	0.12	1.50	1.58	−0.08
3p	1.55	1.51	0.04	2.15	1.89	0.25	1.24	1.20	0.04	1.24	1.19	0.05	1.55	1.78	−0.24	1.55	1.43	0.12

Bold values indicates the activity calculated using the developed QSAR models for compounds for which the antibacterial/antifungal activity has not been determined experimentally.

QSAR model for antibacterial activity against E. coli

$$\text{pMICec} = -0.227\kappa\alpha_2 + 2.569 \quad (3)$$

$$n = 9 \quad r = 0.697 \quad q^2 = 0.268 \quad s = 0.083 \quad F = 6.63$$

The negative correlation of molecular descriptor with antibacterial activity reveals that decrease in value of $\kappa\alpha_2$ (Table 7) will lead to increase in antibacterial activity against *E. coli*.

The model described by Eq. (4) depicted the importance of third order molecular connectivity index, $^3\chi$, in describing the antibacterial activity against *P. aeruginosa*.

QSAR model for antibacterial activity against P. aeruginosa

$$\text{pMICpa} = -0.480\,{}^3\chi + 2.179 \quad (4)$$

$$n = 9 \quad r = 0.883 \quad q^2 = 0.434 \quad s = 0.055 \quad F = 24.78$$

The Eq. (5), derived for the antifungal activity of synthesized 10a-phenylbenzo[*b*]indeno[1,2-*e*][1,4]thiazin-11(10a*H*)-ones (**3a**–**3p**) against *A. fumigates* indicated the importance of the electronic parameter, highest occupied molecular orbital (HOMO) in describing the antifungal activity.

QSAR model for antifungal activity against A. fumigates

$$\text{pMICaf} = -2.421\ \text{HOMO} - 19.118 \quad (5)$$

$$n = 10 \quad r = 0.838 \quad q^2 = 0.401 \quad s = 0.183 \quad F = 18.88$$

The negative correlation of HOMO with antifungal activity against *A. fumigates* reveals that decrease in value of HOMO (Table 7) will lead to increase in antibacterial activity against *A. fumigates*, which can be clearly seen from the results of antifungal activity against *A. fumigates* (Table 6) and values of HOMO presented in Table 7.

The antifungal activity of synthesized 10a-phenylbenzo[*b*]indeno[1,2-*e*][1,4]thiazin-11(10a*H*)-ones (**3a**–**3p**) against *C. albicans* is best described the electronic parameter, dipole moment (μ) (Eq. (6)).

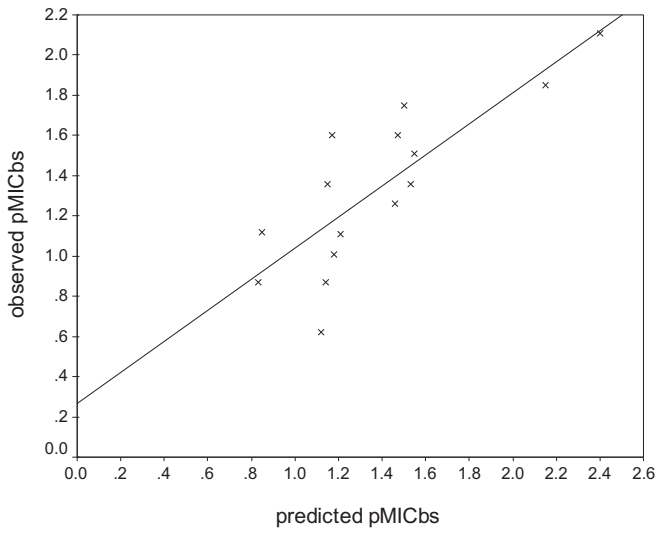

Fig. 5. Plot of predicted pMICbs against the observed pMICbs for the QSAR model developed by Eq. (1).

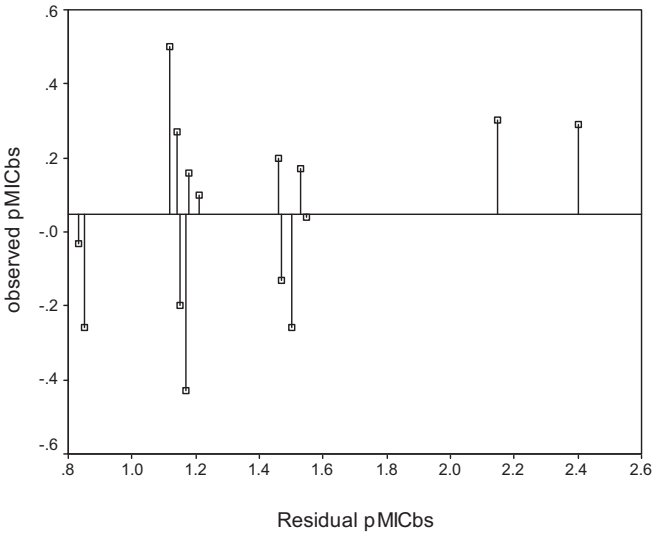

Fig. 6. Plot of residual pMICbs against the observed pMICbs for the QSAR model developed by Eq. (1).

QSAR model for antifungal activity against C. albicans

$$\text{pMICca} = 0.298\,\mu + 0.501 \quad (6)$$

$$n = 9 \quad r = 0.842 \quad q^2 = 0.518 \quad s = 0.133 \quad F = 17.15$$

The coefficient of μ is positive in Eq. (6), which indicates that that the antibacterial activity will increase with the increase in μ of the synthesized compounds, which can be clearly seen from the results of antifungal activity against *C. albicans* (Table 6) and values of dipole moment presented in Table 7.

The importance of dipole moment in modulating antifungal activity against *C. albicans* may be due to the presence of carbonyl group (C^+-O^-) where permanent polarization is seen due to electronegativity difference between the atoms. The carbonyl oxygen of 10a-phenylbenzo[*b*]indeno[1,2-*e*][1,4]thiazin-11(10a*H*)-ones (**3a**–**3p**) may involve in making fruitful binding interactions with amino acid present at the target site, through hydrogen bonding [64].

As in case of Eq. (1), the predictive ability of Eq. (2) to Eq. (6) against respective microorganisms is supported by the low residual activity values (Table 10). Further the high q^2 values observed also supports the suitability of the QSAR models ($q^2 > 0.5$) described by Eqs. (2) and (6). In case of the QSAR models derived for *E. coli*, *P. aeruginosa* and *A. fumigates* (Eqs. (3)–(5)) the q^2 value is less than 0.5, which shows that the developed models are invalid one. But one should not forget the recommendations of Golbraikh and Tropsha [60] who have reported that the only way to estimate the true predictive power of a QSAR model is to test their ability to predict accurately the biological activities of compounds. As the observed and predicted values are close to each other (Table 10), the QSAR models for *E. coli*, *P. aeruginosa* and *A. fumigates* are valid ones.

It is important to note a fact here that the different compounds which are removed as outliers against corresponding microorganisms at the beginning of the study showed high residual values (Table 10) which justified their removal as outliers.

Summarizing, the antibacterial activity of synthesized 10a-phenylbenzo[*b*]indeno[1,2-*e*][1,4]thiazin-11(10a*H*)-ones (**3a**–**3p**) are governed by topological parameters, Kiers second order molecular index ($\kappa\alpha_2$) and molecular connectivity index (χ) in describing the antibacterial activity and electronic parameters, the energy of highest occupied molecular orbital (HOMO) and the dipole moment (μ) in describing the antifungal activity. The importance of topological parameters and electronic parameters in describing the antibacterial and antifungal activity respectively, indicates a fact that different structural requirements are necessary for a compound to be active against bacterial and fungal targets.

Generally for QSAR studies, the biological activities of compounds should span 2–3 orders of magnitude. But in the present study the range of antimicrobial activities of the synthesized compounds is within one order of magnitude. But it is important to note that the predictability of the QSAR models developed in the present study is highly evidenced by the low residual values. This is in accordance with results suggested by the Bajaj et al. [65], who stated that the reliability of the QSAR model lies in its predictive ability even though the activity data are in the narrow range. Further, recent literature reveals that the QSAR have been applied to describe the relationship between narrow range of biological activity and physicochemical properties of the molecules [66–68]. When biological activity data lies in the narrow range, the presence of minimum standard deviation of the biological activity justifies its use in QSAR studies [69,70]. The minimum standard deviation (Table 6) observed in the antimicrobial activity data justifies its use in QSAR studies.

3. Conclusion

In conclusion, we have prepared successfully sixteen new 10a-phenylbenzo[*b*]indeno[1,2-*e*][1,4]thiazin-11(10a*H*)-ones (**3a**–**3p**) using easily obtainable starting compounds under environmentally benign conditions in high yields. The structures of the newly synthesized compounds were established on the basis of different spectral and analytical techniques. The *in vitro* antimicrobial activities of the synthesized compounds were evaluated against various Gram positive, Gram-negative bacteria and fungi. Most of the compounds exhibited convincing biological activities, however, with a degree of variation. Moreover, antibacterial activity was more fruitful than antifungal activity. The QSAR study carried out to find the relationship between physicochemical parameters and antimicrobial activity of 10a-phenylbenzo[*b*]indeno[1,2-*e*][1,4]thiazin-11(10a*H*)-ones (**3a**–**3p**) indicated the importance of topological parameters, Kiers second order molecular index ($\kappa\alpha_2$) and molecular connectivity index (χ) in describing the antibacterial activity and electronic parameters, the energy of highest occupied molecular orbital (HOMO) and the dipole moment (μ) in describing the antifungal activity.

4. Experimental

4.1. Chemistry

Melting points were determined in open capillaries and are uncorrected. The purity of synthesized compounds was tested using precoated TLC plates (SIL G/UV_{254}, ALUGRAM) and visualization was achieved via UV. The IR absorption spectra were recorded on Perkin Elmer Spectrum, BX II FTIR spectrometer, using (KBr) pellets and absorption frequencies (ν) are stated in cm^{-1}. The ^1H, ^{13}C NMR spectra (DMSO-d_6/$CDCl_3$) were measured on Bruker Advance 300/400 MHz and 75/100 MHz respectively. The chemical shifts are expressed in parts per million (δ ppm). Tetramethylsilane (TMS) was used as an internal standard. Coupling constants (J) were measured in Hz. Mass spectra were recorded on Agilent 6310 LCMS ION TRAP. Elemental analysis was carried out using Vario Micro Cube Elementar CHNS analyser. Analytical results for C, H, N and S were within ±0.4% of the theoretical values. Solvents were dried as per literature procedures. Penicillin, streptomycin (Hi-Media) and fluconazole (Aurobindo Pharmaceuticals Pvt. Ltd, Mandal, A.P., India) were respectively used as standard antibacterial and antifungal agents against microorganisms studied.

4.2. General procedure for the synthesis of 2-arylindan-1,3-diones

The 2-arylindan-1,3-diones needed for the purpose were prepared by condensation of phthalide with appropriate *p*-substituted benzaldehydes in the presence of an alkoxide and ester in high yields according to the procedure as described in the literature [36,37].

4.3. General procedure for the synthesis of 2-bromo-2-arylindan-1,3-diones (*1*)

The 2-bromo-2-arylindan-1,3-diones (**1**) were obtained by bromination of 2-arylindan-1,3-diones in chloroform as described in the literature [35].

4.4. General procedure for the synthesis of 5-substituted-2-aminobenzenethiols (*2*)

The 5- substituted-2-aminobenzenethiols (**2**) were derived from base catalyzed hydrolytic fission of 6-substituted-2-

aminobenzothiazoles which, in turn, were prepared by action of potassium thiocyanate and bromine (generating thiocyanogen, [$(SCN)_2$], *in situ*) on *p*-substituted anilines as described in the literatures [38–40].

4.5. General procedure for the synthesis of 10a-phenylbenzo[b]indeno[1,2-e][1,4]thiazin-11(10aH)-ones (**3**)

A solution of 2-bromo-2-phenyl/*p*-substituted phenylindan-1,3-dione (**1**) (3 mmol) and 2-aminobenzenethiol/2-amino-5-substituted benzenethiol (**2**) (3 mmol) in 30 mL of dry ethanol was refluxed on a water bath for 5–8 h. The solid so obtained was filtered which upon recrystallization furnished **3a**–**3p** in high yields (70–84%). The spectral and analytical data of **3a**–**3p** are given as follows:

4.5.1. 10a-Phenylbenzo[b]indeno[1,2-e][1,4]thiazin-11(10aH)-one (**3a**)

Yellow crystals (ethanol), yield 0.756 g (77%); mp 190 °C; IR (KBr): 3069–3000 (Ar–CH), 1696 (C=O), 1606 (C=N) cm^{-1}; ^1H NMR ($CDCl_3$): δ 9.18 (1H, d, $J = 8.4$ Hz, H-6), 7.93 (1H, d, $J = 7.5$ Hz, H-1), 7.53–7.22 (8H, m, H-2, H-3, H-4, H-7, H-3′, H-4′, H-5′, H-6′), 7.07 (2H, d, $J = 8.4$ Hz, H-8, H-9), 6.48 (1H, d, $J = 8.1$ Hz, H-2′); ^{13}C NMR ($CDCl_3$): δ 182.34, 165.21, 134.68, 133.88, 131.46, 130.82, 129.84, 129.62, 129.47, 128.35, 128.26, 127.70, 126.80, 125.45, 125.40, 123.02, 121.85, 119.99, 119.39, 118.34; ESI-MS *m*/*z*: $(M + H)^+$ 328; *Anal.* Calcd. for $C_{21}H_{13}NOS$ (327.07): C, 77.04; H, 4.00; N, 4.28; S, 9.79. Found: C, 76.94; H, 3.87; N, 4.21; S, 9.71.

4.5.2. 8-Methyl-10a-phenylbenzo[b]indeno[1,2-e][1,4]thiazin-11(10aH)-one (**3b**)

Yellow solid (benzene), yield 0.819 g (80%); mp 258–260 °C; IR (KBr): 3070–3015 (Ar–CH), 2990–2914 (aliph.–CH), 1687 (C=O), 1598 (C=N) cm^{-1}; ^1H NMR ($CDCl_3$): δ 9.10 (1H, d, $J = 9.0$ Hz, H-6), 7.94 (1H, d, $J = 7.5$ Hz, H-1), 7.56–7.26 (8H, m, H-2, H-3, H-4, H-7, H-3′, H-4′, H-5′, H-6′), 7.21 (1H, d, $J = 2.4$ Hz, H-9), 6.48 (1H, d, $J = 8.1$ Hz, H-2′), 2.30 (3H, s); ^{13}C NMR ($CDCl_3$): δ 184.22, 165.20, 135.63, 135.30, 134.61, 131.37, 130.78, 130.47, 130.08, 129.84, 129.52, 128.43, 128.23, 127.10, 126.75, 125.73, 123.13, 121.86, 119.64, 118.35, 20.54; ESI-MS *m*/*z*: $(M + H)^+$ 342; *Anal.* Calcd. for $C_{22}H_{15}NOS$ (341.09): C, 77.39; H, 4.43; N, 4.10; O, 4.69; S, 9.39. Found: C, 77.25; H, 4.56; N, 3.95; S, 9.21.

4.5.3. 8-Methoxy-10a-phenylbenzo[b]indeno[1,2-e][1,4]thiazin-11(10aH)-one (**3c**)

Greenish yellow solid (benzene), yield 0.798 g (74.5%); mp 224–225 °C; IR (KBr): 3068–3010 (Ar–CH), 2985–2915 (aliph.–CH), 1689 (C=O), 1602 (C=N) cm^{-1}; ^1H NMR ($CDCl_3$): δ 9.17 (1H, d, $J = 9.6$, H-6), 7.93 (1H, d, $J = 7.6$ Hz, H-1), 7.53–6.81 (8H, m, H-2, H-3, H-4, H-7, H-3′, H-4′, H-5′, H-6′), 6.69 (1H, d, $J = 2.8$ Hz, H-9), 6.47 (1H, d, $J = 8.0$ Hz, H-2′), 3.88 (3H, s); ^{13}C NMR ($CDCl_3$): δ 184.40, 164.88, 156.52, 134.61, 131.26, 130.71, 129.89, 129.65, 129.56, 128.48, 128.29, 127.23, 126.87, 122.87, 121.85, 121.27, 120.61, 117.64, 112.52, 110.68, 55.55; ESI-MS *m*/*z*: $(M + H)^+$ 358.1; *Anal.* Calcd. for $C_{22}H_{15}NO_2S$ (357.08): C, 73.93; H, 4.23; N, 3.92; S, 8.97. Found: C, 73.93; H, 4.11; N, 3.81; S, 8.83.

4.5.4. 8-Bromo-10a-phenylbenzo[b]indeno[1,2-e][1,4]thiazin-11(10aH)-one (**3d**)

Green crystals (ethanol), yield 0.996 g (82%); mp 268–270 °C; IR (KBr): 3066–3010 (Ar–CH), 1690 (C=O), 1603 (C=N) cm^{-1}; ^1H NMR ($CDCl_3$): δ 9.10 (1H, d, $J = 9.0$ Hz, H-6), 7.93 (1H, d, $J = 7.5$ Hz, H-1), 7.55–7.06 (8H, m, H-2, H-3, H-4, H-7, H-3′, H-4′, H-5′, H-6′), 6.90 (1H, d, $J = 2.4$ Hz, H-9), 6.46 (1H, d, $J = 8.1$ Hz, H-2′); ^{13}C NMR ($CDCl_3$): δ 184.14, 165.20, 135.61, 134.19, 132.97, 131.75, 130.79, 130.48, 130.08, 129.76, 129.47, 128.57, 128.17, 127.70, 123.14, 122.34, 121.97, 120.64, 117.95, 110.23; ESI-MS *m*/*z*: $(M)^+$ 405, $(M + H)^+$ 406, $(M + 2)^+$ 407; *Anal.* Calcd. for $C_{21}H_{12}BrNOS$ (404.98): C, 62.08; H, 2.98; N, 3.45; S, 7.89. Found: C, 61.92; H, 2.81; N, 3.68; S, 7.73.

4.5.5. 10a-(p-Tolyl)benzo[b]indeno[1,2-e][1,4]thiazin-11(10aH)-one (**3e**)

Yellow solid (ethanol), yield 0.788 g (77%); mp 170 °C; IR (KBr): 3085–3017 (Ar–CH), 2983–2913 (aliph.–CH), 1694 (C=O), 1610 (C=N) cm^{-1}; ^1H NMR (DMSO-d_6): δ 9.03 (1H, d, $J = 8.4$ Hz, H-6), 7.86 (1H, d, $J = 7.6$ Hz, H-1), 7.51–7.26 (7H, m, H-2, H-3, H-4, H-7, H-3′, H-5′, H-6′), 7.17 (2H, d, $J = 8.4$ Hz, H-8, H-9), 6.49 (1H, d, $J = 8.0$ Hz, H-2′); 2.49 (3H, s); ^{13}C NMR (DMSO-d_6): δ 183.82, 164.67, 140.38, 133.60, 132.56, 131.48, 130.88, 130.75, 129.49, 129.28, 128.77, 128.28, 127.88, 126.44, 126.36, 123.25, 121.90, 119.74, 118.96, 118.32, 21.51; ESI-MS *m*/*z*: $(M + H)^+$ 342; *Anal.* Calcd. for $C_{22}H_{15}NOS$ (341.09): C, 77.39; H, 4.43; N, 4.10; S, 9.39. Found: C, 77.25; H, 4.32; N, 4.01; S, 9.23.

4.5.6. 8-Methyl-(p-tolyl)benzo[b]indeno[1,2-e][1,4]thiazin-11(10aH)-one (**3f**)

Yellow solid (benzene), yield 0.884 g (83%); mp 168–170 °C; IR (KBr): 3072–3005 (Ar–CH), 2988–2925 (aliph.–CH), 1697 (C=O), 1614 (C=N) cm^{-1}; ^1H NMR ($CDCl_3$): δ 9.10 (1H, d, $J = 8.9$ Hz, H-6), 7.83 (1H, d, $J = 7.42$ Hz, H-1), 7.60–7.21 (7H, m, H-2, H-3, H-4, H-7, H-3′, H-5′, H-6′), 7.17 (1H, d, 2.8 Hz, H-9), 6.52 (1H, d, $J = 8.1$ Hz, H-2′), 2.46 (6H, s); ^{13}C NMR ($CDCl_3$): δ 183.75, 162.23, 140.23, 139.52, 136.31, 133.15, 132.23, 131.72, 130.95, 130.62, 130.10, 129.65, 128.23, 127.62, 126.32, 126.12, 123.96, 121.46, 118.38, 117.95, 21.58, 20.58; ESI-MS *m*/*z*: $(M + H)^+$ 356; *Anal.* Calcd. for $C_{23}H_{17}NOS$ (355): C, 77.72; H, 4.82; N, 3.94; S, 9.02. Found: C, 77.69; H, 4.67; N, 3.97; S, 8.95.

4.5.7. 8-Methoxy-10a-(p-tolyl)benzo[b]indeno[1,2-e][1,4]thiazin-11(10aH)-one (**3g**)

Greenish yellow solid (benzene), yield 0.700 g (74%); mp 192 °C; IR (KBr): 3066–3013 (Ar–CH), 2988–2928 (aliph.–CH), 1684 (C=O), 1604 (C=N) cm^{-1}; ^1H NMR ($CDCl_3$): δ 9.17 (1H, d, $J = 9.2$ Hz, H-6), 7.92 (1H, d, $J = 7.6$ Hz, H-1), 7.44–6.78 (7H, m, H-2, H-3, H-4, H-7, H-3′, H-5′, H-6′), 6.62 (1H, d, $J = 2.8$ Hz, H-9), 6.56 (1H, d, $J = 8.0$ Hz, H-2′), 3.80 (3H, s), 2.48 (3H, s); ^{13}C NMR ($CDCl_3$): δ 183.90, 164.85, 156.48, 139.98, 131.58, 131.20, 130.77, 130.32, 129.35, 128.43, 128.35, 128.19, 127.23, 126.74, 122.81, 121.92, 121.39, 120.58, 117.87, 112.47, 55.53, 21.57; ESI-MS *m*/*z*: $(M + Na)^+$ 394.4; *Anal.* Calcd. for $C_{23}H_{17}NO_2S$ (371.10): C, 74.37; H, 4.61; N, 3.77; S, 8.63. Found: C, 74.50; H, 4.48; N, 3.62; S, 8.51.

4.5.8. 8-Bromo-10a-(p-tolyl)benzo[b]indeno[1,2-e][1,4]thiazin-11(10aH)-one (**3h**)

Greenish yellow crystals (benzene), yield 1.056 g (84%); mp 280 °C; IR (KBr): 3096–3010 (Ar–CH), 2996–2928 (aliph.–CH), 1682 (C=O), 1598 (C=N) cm^{-1}; ^1H NMR ($CDCl_3$): δ 9.09 (1H, d, $J = 9.0$ Hz, H-6), 7.93 (1H, d, $J = 7.8$ Hz, H-1), 7.46–7.26 (7H, m, H-2, H-3, H-4, H-7, H-3′, H-5′, H-6′), 7.20 (1H, d, $J = 2.1$ Hz, H-9), 6.57 (1H, d, $J = 7.8$ Hz, H-2′), 2.48 (3H, s); ^{13}C NMR ($CDCl_3$): δ 183.78, 165.19, 140.23, 136.43, 132.94, 131.96, 131.69, 131.15, 130.84, 130.38, 129.26, 128.46, 128.10, 127.65, 126.85, 126.60, 123.07, 122.03, 118.96, 117.89, 21.58; ESI-MS *m*/*z*: $(M)^+$ 419.2, $(M + H)^+$ 420.5, $(M + 2)^+$ 421.8; *Anal.* Calcd. for $C_{22}H_{14}BrNOS$ (419.00): C, 62.87; H, 3.36; N, 3.33; S, 7.63. Found: C, 62.69; H, 3.25; N, 3.18; S, 7.81.

4.5.9. 10a-(4-Methoxyphenyl)benzo[b]indeno[1,2-e][1,4]thiazin-11(10aH)-one (**3i**)

Yellow crystals (DMSO), yield 0.772 g (72%); mp 180–182 °C; IR (KBr): 3072–3018 (Ar–CH), 2963–2913 (aliph.–CH), 1697 (C=O),

1603 (C=N) cm^{-1}; ^1H NMR (DMSO-d_6): δ 9.04 (1H, d, J = 8.4 Hz, H-6), 7.87 (1H, d, J = 7.6 Hz, H-1), 7.66–7.27 (7H, m, H-2, H-3, H-4, H-7, H-3′, H-5′, H-6′), 7.13 (2H, d, J = 8.4 Hz, H-8, H-9), 6.94 (1H, d, J = 7.9 Hz, H-2′), 3.85 (3H, s); ^{13}C NMR (DMSO-d_6): δ 184.25, 164.70, 160.94, 133.61, 132.62, 131.48, 131.11, 130.82, 129.26, 128.27, 127.87, 126.56, 126.34, 126.25, 124.15, 123.25, 121.96, 121.81, 119.86, 55.58; ESI-MS m/z: $(M + H)^+$ 358; *Anal*. Calcd. for $C_{22}H_{15}NO_2S$ (357.08): C, 73.93; H, 4.23; N, 3.92; S, 8.97. Found: C, 73.81; H, 4.10; N, 3.71; S, 8.73.

4.5.10. 10a-(4-Methoxyphenyl)-8-methylbenzo[b]indeno[1,2-e][1,4] thiazin-11(10aH)-one (**3j**)

Orange yellow solid (DMSO), yield 0.813 g (73%); mp 220–222 °C; IR (KBr): 3075–3021 (Ar–CH), 2993–2920 (aliph.–CH), 1684 (C=O), 1615 (C=N) cm^{-1}; ^1H NMR ($CDCl_3$): δ 9.06 (1H, d, J = 8.6 Hz, H-6), 7.82 (1H, d, J = 7.3 Hz, H-1), 7.53–7.27 (7H, m, H-2, H-3, H-4, H-7, H-3′, H-5′, H-6′), 7.21 (1H, d, J = 2.8 Hz, H-9), 6.65 (1H, d, J = 7.6 Hz, H-2′), 3.88 (3H, s), 2.49 (3H, s); ^{13}C NMR ($CDCl_3$): δ 184.67, 165.07, 160.70, 135.24, 134.38, 131.30, 130.85, 130.00, 128.42, 128.28, 128.12, 126.80, 125.68, 123.08, 122.92, 121.90, 119.85, 119.51, 119.24, 115.01, 55.43, 20.65; ESI-MS m/z: $(M + H)^+$ 372; *Anal*. Calcd. for $C_{23}H_{17}NO_2S$ (371.10): C, 74.37; H, 4.61; N, 3.77; S, 8.63. Found: C, 74.25; H, 4.72; N, 3.60; S, 8.41.

4.5.11. 8-Methoxy-10a-(4-methoxyphenyl)benzo[b]indeno[1,2-e] [1,4]thiazin11(10aH)-one (**3k**)

Greenish yellow solid (benzene), yield 0.813 g (70%); mp 196–198 °C; IR (KBr): 3069–3034 (Ar–CH), 2978–2906 (aliph.–CH), 1685 (C=O), 1601 (C=N) cm^{-1}; ^1H NMR ($CDCl_3$): δ 9.13 (1H, d, J = 9.1 Hz, H-6), 7.91 (1H, d, J = 7.6 Hz, H-1), 7.45–7.24 (7H, m, H-2, H-3, H-4, H-7, H-3′, H-5′, H-6′), 6.81 (1H, d, J = 2.7 Hz, H-9), 6.54 (1H, d, J = 8.1 Hz, H-2′), 3.80 (6H, s); ^{13}C NMR ($CDCl_3$): δ 184.92, 164.28, 159.60, 156.60, 136.60, 134.71, 132.85, 131.15, 130.61, 130.42, 130.03, 129.42, 127.11, 126.02, 122.96, 115.85, 115.18, 115.01, 113.01, 112.48, 55.60, 55.48; ESI-MS m/z: $(M + H)^+$ 388; *Anal*. Calcd. for $C_{23}H_{17}NO_3S$ (387.09): C, 71.30; H, 4.42; N, 3.62; S, 8.28. Found: C, 71.45; H, 4.30; N, 3049; S, 8.16.

4.5.12. 8-Bromo-10a-(4-methoxyphenyl)benzo[b]indeno[1,2-e][1,4] thiazin-11(10aH)-one (**3l**)

Light green crystals (benzene), yield 0.992 g (76%); mp 251–253 °C; IR (KBr): 3062–3029 (Ar–CH), 2980–2915 (aliph.–CH), 1692 (C=O), 1598 (C=N) cm^{-1}; ^1H NMR ($CDCl_3$): δ 9.10 (1H, d, J = 9.2 Hz, H-6), 7.93 (1H, d, J = 7.2 Hz, H-1), 7.58–7.27 (7H, m, H-2, H-3, H-4, H-7, H-3′, H-5′, H-6′), 7.20 (1H, d, J = 2.8 Hz, H-9), 6.57 (1H, d, J = 7.6 Hz, H-2′), 3.88 (3H, s); ^{13}C NMR ($CDCl_3$): δ 184.70, 165.81, 159.53, 136.88, 133.61, 131.20, 130.95, 130.48, 130.01, 129.72, 128.56, 128.01, 127.73, 126.43, 125.85, 123.01, 121.96, 120.02, 114.98, 113.45, 55.55; ESI-MS m/z: $(M)^+$ 435.4, $(M + H)^+$ 436.2, $(M + 2)^+$ 437; *Anal*. Calcd. for $C_{22}H_{14}BrNO_2S$ (434.99): C, 60.56; H, 3.23; N, 3.21; S, 7.35. Found: C, 60.43; H, 3.31; N, 31.93; S, 7.15.

4.5.13. 10a-(4-Chlorophenyl)benzo[b]indeno[1,2-e][1,4]thiazin-11(10aH)-one (**3m**)

Yellow crystals (benzene), yield 0.844 g (78%); mp 210 °C; IR (KBr): 3061–3013 (Ar–CH), 1688 (C=O), 1598 (C=N) cm^{-1}; ^1H NMR ($CDCl_3$): δ 9.19 (1H, d, J = 8.1 Hz, H-6), 7.95 (1H, d, J = 7.2 Hz, H-1), 7.56–7.24 (7H, m, H-2, H-3, H-4, H-7, H-3′, H-5′, H-6′), 7.09 (2H, d, J = 8.1 Hz, H-8, H-9), 6.48 (1H, d, J = 7.5 Hz, H-2′); ^{13}C NMR ($CDCl_3$): δ 184.35, 164.60, 134.09, 133.59, 133.16, 131.48, 130.70, 130.25, 129.49, 129.28, 128.28, 127.87, 126.43, 126.36, 126.01, 124.13, 122.56, 120.43, 119.43, 118.01; ESI-MS m/z: $(M)^+$ 361, $(M + 1)^+$ 362, $(M + 2)^+$ 363; *Anal*. Calcd. for $C_{21}H_{12}ClNOS$ (361.03): C, 69.71; H, 3.34; N, 3.87; S, 8.86. Found: C, 69.58; H, 3.21; N, 3.62; S, 8.71.

4.5.14. 10a-(4-Chlorophenyl)-8-methylbenzo[b]indeno[1,2-e][1,4] thiazin-11(10aH)-one (**3n**)

Yellow crystals (ethanol), yield 0.922 g (82%); mp 250–250 °C; IR (KBr): 3080–3010 (Ar–CH), 2990–2915 (aliph.–CH), 1682.96 (C=O), 1602.43 (C=N) cm^{-1}; ^1H NMR ($CDCl_3$): δ 9.08 (1H, d, J = 8.4 Hz, H-6), 7.94 (1H, d, J = 7.8 Hz, H-1), 7.56–7.23 (7H, m, H-2, H-3, H-4, H-7, H-3′, H-5′, H-6′), 7.05 (1H, d, J = 2.1 Hz, H-9), 6.47 (1H, d, J = 8.1 Hz, H-2′), 2.30 (3H, s); ^{13}C NMR ($CDCl_3$): δ 184.42, 165.09, 140.23, 136.27, 135.32, 134.75, 131.35, 130.78, 129.84, 129.64, 129.52, 128.43, 128.37, 128.24, 126.75, 125.74, 122.95, 121.86, 119.65, 113.72, 20.56; ESI-MS m/z: $(M)^+$ 375, $(M + 1)^+$ 376, $(M + 2)^+$ 377; *Anal*. Calcd. for $C_{22}H_{14}ClNOS$ (375.05): C, 70.30; H, 3.75; N, 3.73; S, 8.53. Found: C, 70.15; H, 3.92; N, 3.66; S, 8.31.

4.5.15. 10a-(4-Chlorophenyl)-8-methoxybenzo[b]indeno[1,2-e][1,4] thiazin-11(10aH)-one (**3o**)

Orange yellow crystals (benzene), yield 0.880 g (75%); mp 225 °C; IR (KBr): 3073–3000 (Ar–CH), 2996–2900 (aliph.–CH), 1688 (C=O), 1600.02 (C=N) cm^{-1}; ^1H NMR ($CDCl_3$): δ 9.15 (1H, d, J = 9.6 Hz, H-6), 7.93 (1H, d, J = 7.6 Hz, H-1), 7.54–6.78 (7H, m, H-2, H-3, H-4, H-7, H-3′, H-5′, H-6′), 6.62 (1H, d, J = 2.0 Hz, H-9), 6.55 (1H, d, J = 7.6 Hz, H-2′), 3.81 (3H, s); ^{13}C NMR ($CDCl_3$): δ 184.72, 164.81, 156.58, 136.81, 136.00, 133.07, 131.41, 131.11, 130.52, 130.03, 128.55, 127.19, 127.11, 123.02, 121.71, 120.93, 120.62, 116.12, 112.61, 110.70, 55.55; ESI-MS m/z: $(M)^+$ 391.2, $(M + H)^+$ 392; *Anal*. Calcd. for $C_{22}H_{14}ClNO_2S$ (391.04): C, 67.43; H, 3.60; N, 3.57; S, 8.18. Found: C, 67.28; H, 3.71; N, 3.40; S, 8.01.

4.5.16. 8-Bromo-10a-(4-chlorophenyl)benzo[b]indeno[1,2-e][1,4] thiazin-11(10aH)-one (**3p**)

Yellow solid, yield 1.093 g (83%); mp 261–264 °C; IR (KBr): 3080–3010 (Ar–CH), 1693.57 (C=O), 1596.16 (C=N) cm^{-1}, ^1H NMR($CDCl_3$): δ 9.07 (1H, d, J = 9.0 Hz, H-6), 7.94 (1H, d, J = 7.5 Hz, H-1), 7.55–7.26 (7H, m, H-2, H-3, H-4, H-7, H-3′, H-5′, H-6′), 7.20 (1H, d, J = 2.1 Hz, H-9), 6.56 (1H, d, 7.8 Hz, H-2′); ^{13}C NMR ($CDCl_3$): δ 184.57, 165.21, 140.10, 136.23, 133.02, 132.66, 131.90, 131.01, 130.60, 130.14, 128.82, 128.24, 127.72, 127.08, 126.15, 123.30, 121.83, 120.65, 118.05, 116.07; ESI-MS m/z: $(M)^+$ 439, $(M + 1)^+$ 440.3, $(M + 2)^+$ 441.1; *Anal*. Calcd. for $C_{21}H_{11}BrClNOS$ (438.94): C, 57.23; H, 2.52; N, 3.18; S, 7.28. Found: C, 57.14; H, 2.31; N, 3.01; S, 7.10.

4.6. Antibacterial activity

The *in vitro* antibacterial activity of the sixteen synthesized compounds **3a**–**3p** were tested against two Gram-positive bacteria *viz. B. subtilis* (MTCC 441), *S. aureus* (MTCC 7443) and two Gram-negative bacteria *viz. E. coli* (MTCC 42), *P. aeruginosa* (MTCC 7952). Initially, weighed amounts of synthesized compounds were dissolved in DMSO (1.0 mg of the test compound in 10 mL DMSO) to prepare stock solutions. After that they were diluted to a final concentration of 100 μg/mL in Luria broth media. From this serial two-fold dilutions were prepared in the range of 100–1.56 μg/mL. Penicillin and Streptomycin were taken as reference compounds and DMSO as a negative control. Respective Gram-positive bacteria *B. subtilis* and *S. aureus* and Gram-negative bacteria *E. coli* and *P. aeruginosa* were grown in Luria broth media at 37 °C and harvested with centrifugation. Bacteria were given three times wash with Phosphate buffer saline. Then 100 μL of the broth containing test bacteria were inoculated to different dilutions of test compounds in each well of a 96-well plate (each dilution in triplicates). The inoculated plates were incubated for 24 h at 37 °C. After 24 h bacterial growth was monitored visually and spectrophotometrically. The reference compounds penicillin and streptomycin were also assessed under similar conditions for comparison with the compounds synthesized.

4.7. Antifungal activity

The *in vitro* antifungal activity of the sixteen synthesized compounds **3a**–**3p** were tested against two fungi *A. fumigates* (MTCC 2550) and *C. albicans* (MTCC 183). The pattern which was used for screening bacteria was translated exactly for antifungal activity. Initially, weighed amounts of the synthesized compounds were dissolved in DMSO (1.0 mg of the test compound in 10 mL DMSO) to prepare stock solutions. After that they were diluted to a final concentration of 100 μg/mL in Potato dextrose broth media. From this serial two-fold dilutions were prepared in the range of 100 to 1.56 μg/mL. Fluconazole was used as reference against fungi and DMSO as a negative control. Fungal samples, *A. fumigates* and *C. albicans* were grown on Sabouraud dextrose broth media at 28 °C for 2–3 weeks and for 48 h respectively. Fungal spores were harvested by centrifugation, and washed with sterile distilled water. Then 100 μL of the broth containing test fungi were inoculated to different dilutions of test compounds in each well of a 96-well plate (each dilution in triplicates) and incubated for 72 h at 28 °C. Finally, the Minimum Inhibitory Concentration (MIC) was assigned by CFU assay. Antifungal activity of the reference drug, Fluconazole was also assessed under similar conditions.

4.8. QSAR studies

4.8.1. Data set

In the present work, the antimicrobial activity of 10a-phenylbenzo[*b*]indeno[1,2-*e*][1,4]thiazin-11(10a*H*)-one derivatives (**3a**–**3p**) was subjected to MLR analysis with their physicochemical properties.

4.8.2. Descriptor generation

The next step in developing the QSAR model is generation of the numerical descriptors encoding the structural features of the molecules such as hydrophobic, geometric, electronic and topological characters. The structures of 10a-phenylbenzo[*b*]indeno[1,2-*e*][1,4]thiazin-11(10a*H*)-ones (**3a**–**3p**) were first pre-optimized with the Molecular Mechanics Force Field (MM+) procedure included in Hyperchem 6.03 [71] and the resulting geometries are further refined by means of the semiempirical method PM3 (parametric Method-3). We chose a gradient norm limit of 0.01 kcal/Å for the geometry optimization. The different molecular descriptors (independent variables) like log of octanol–water partition coefficient (log *P*), molar refractivity (MR), Kier's molecular connectivity ($^{n}\chi$, $^{n}\chi^{v}$) and shape (κ_n, $\kappa\alpha_n$) topological indices, Randic topological index (R), Balaban topological index (J), Wiener topological index (W), Total energy (Te), energies of highest occupied molecular orbital (HOMO) and lowest unoccupied molecular orbital (LUMO), dipole moment (μ), electronic energy (Ele.E), nuclear energy (Nu.E) and molecular surface area (SA) calculated for the synthesized 10a-phenylbenzo[*b*]indeno[1,2-*e*][1,4]thiazin-11(10a*H*)-ones (**3a**–**3p**) [53–58] using the software TSAR 3.3 [72]. Since, there were a large number of descriptors for each compound, we used Pearson's correlation matrix as a qualitative model, in order to select the suitable descriptors for MLR analysis. The stepwise multiple linear regression procedure was used for model generation. The stepwise addition method implemented in the SPSS software package (SPSS for windows, Version 10.05 1999) was used for choosing the descriptors contributing to the antimicrobial activity. Further, the regression analysis was performed using the SPSS software package [73].

4.8.3. Cross validation

The predictive powers of the equation were validated by determination of cross-validated r^2 (q^2) using leave one out (LOO) cross-validation method [74], where a model is built with *N*- 1 compounds and the *N*th compound is predicted. Each compound is left out of the model derivation and predicted in turn. An indication of the performance of the model is obtained from the cross-validated (or predictive q^2) method, which is defined as,

$$q^2 = (\mathrm{SD} - \mathrm{PRESS}/\mathrm{SD}).$$

Where, SD is the sum of squares deviation for each activity from the mean. PRESS (predictive sum-of-squares) is the sum of the squared difference between the actual and that of the predicted values when the compound is omitted from the fitting process. The model with high q^2 value is said to have high predictability.

Acknowledgements

We are grateful to CSIR, New Delhi for providing financial support [File no. 09/752(0012)/2007-EMR-1] and Institute of Nuclear Medicine and Sciences (INMAS), D.R.D.O., New Delhi, India for NMR and Mass Spectra.

Appendix A. Supplementary data

Supplementary data related to this article can be found online at doi:10.1016/j.ejmech.2012.03.054.

References

[1] S.J. Teague, A.M. Davis, P.D. Leeson, T. Oprea, Angew. Chem. Int. Ed. 38 (1999) 3743–3748.
[2] J.V. Cecchetti, V. Calderone, O. Tabarrini, S. Sabatini, E. Filipponi, L. Testai, R. Spogli, E. Martinotti, A. Fravolini, J. Med. Chem. 46 (2003) 3670–3679.
[3] T. Matasui, Y. Nakamura, H. Ishikawa, A. Matsuura, F. Kobayashi, Jpn. J. Pharmacol. 64 (1994) 115–124.
[4] U.R. Pratap, D.V. Jawale, B.S. Londhe, R.A. Mane, J. Mol. Catal. B: Enzym. 68 (2011) 94–97.
[5] P.I. Williams, M. Smith, Eur. J. Anaesthesiol. 16 (1999) 638–645.
[6] M. Fujita, S. Ito, A. Ota, N. Kato, K. Yamamoto, Y. Kawashima, H. Yamauchi, J. Iwao, J. Med. Chem. 33 (1990) 1898–1905.
[7] B. Baghernejad, M.M. Heravi, H.A. Oskooie, Synth. Commun. 41 (2011) 589–593.
[8] M.K. Nyati, C.M. Rajoria, R.R. Gupta, P.K. Dev, Anti-cancer Drugs 6 (1995) 693–696;
Chem. Abstr. 124 (1996) 21034h.
[9] R.C. Millonig, M.B. Goldlust, W.E. Maguire, B. Rubin, E. Schulze, R.J. Wojnar, A.R. Turkheimer, W.F. Schreiber, R.J. Brittain, J. Med. Chem. 16 (1973) 780–782.
[10] S. Sabatini, G.W. Kaatz, G.M. Rossolini, D. Brandini, A. Fravolini, J. Med. Chem. 51 (2008) 4321–4330;
Chem. Abstr. 86 (1977) 106504h.
[11] V. Cecchetti, A. Fravolini, F. Schiaffella, O. Tabarrini, W. Zhou, P.G. Pagella, J. Heterocycl. Chem. 29 (1992) 375–382.
[12] M.K. Schwarz, D. Tumelty, M.A. Gallop, J. Org. Chem. 64 (1999) 2219–2231.
[13] V. Calderone, R. Spogli, A. Martelli, G. Manfroni, L. Testai, S. Sabatini, T. Oriana, V. Cecchetti, J. Med. Chem. 51 (2008) 5085–5092.
[14] E.V. Nosova, G.N. Lipunova, V.N. Charushin, O.N. Chupakhin, J. Fluor. Chem. 131 (2010) 1267–1288.
[15] T. Kuroita, N. Marubayashi, M. Sano, K. Kanzaki, K. Inaba, T. Kawakita, Chem. Pharm. Bull. (Tokyo) 44 (1996) 2051–2060.
[16] S.N. Pandeya, D. Sriram, E.De. Clercq, G. Nath, Arzneim. Forsch. 50 (2000) 55–59.
[17] G. Grandolini, V. Ambrogi, L. Baiocchi, M. Giannangeli, A. Furlani, A. Papaioannou, L. Perioli, V. Scarcia, Heterocycl. Commun. 1 (1995) 265–280.
[18] T. Yamamoto, M. Hori, I. Watanabe, K. Harada, S. Ikeda, H. Ohtaka, Chem. Pharm. Bull. 48 (2000) 843–849.
[19] J.W. Constantine, I.M. Purcell, J. Pharmacol. Exp. Ther. 187 (1973) 653–665.
[20] M. Bakavoli, H. Sadeghian, Z. Tabatabaei, E. Rezaei, M. Rahimizadeh, M. Nikpour, J. Mol. Model. 14 (2008) 471–478;
Chem. Abstr. 136 (2002) 340675n.
[21] A. Napolitano, S. Memoli, G. Prota, J. Org. Chem. 64 (1999) 3009–3011.
[22] S. Aloui, I. Forsal, M. Sfaira, M.E. Touhami, M. Taleb, M.F. Baba, M. Daoudi, Portu. Electrochim. Acta 27 (2009) 599–613.
[23] R. Mannhold, Med. Chem. Rev. 24 (2004) 213–266.
[24] M. Kumar, K. Sharma, R.M. Samarth, A. Kumar, Eu. J. Med. Chem. 45 (2010) 4467–4472.
[25] Y.T. Ma, M.C. Huang, F.L. Hsu, H.F. Chang, Phytochemistry 48 (1998) 1083–1085.

[26] R. Podsiadły, J. Photochem. Photobiol. A: Chem. 208 (2009) 147–153.
[27] C. Brown, R.M. Davidson, Adv. Heterocycl. Chem. 38 (1985) 135–176.
[28] G. Liso, G. Trapani, V. Berardi, A. Latrofa, P. Marchini, J. Heterocycl. Chem. (1980) 793–796.
[29] E.L. Patmore, H. Chafetz, J. Org. Chem. 32 (1967) 1254–1255.
[30] A.R. Katritzky, C.W. Rees, E.F.V. Scriven, Comprehensive Heterocyclic Chemistry II, Elsevier, Amsterdam, 1996.
[31] B.S. Rathore, M. Kumar, Bioorg. Med. Chem. 14 (2006) 5678–5682.
[32] P.R. Sharma, V. Gupta, D.C. Gautam, R.R. Gupta, Phosphorus Sulfur Silicon 178 (2003) 1483–1488.
[33] A.C. Bajji, S. Nanya, Y. Butsugan, J. Heterocycl. Chem. 30 (1993) 361–363.
[34] J. Mungalpara, A. Pandey, V. Jain, C.G. Mohan, J. Mol. Model. 16 (2010) 629–644.
[35] G. Vanags, A. Arens, Zhur. Obsh. Khim. 27 (1957) 1358; Chem. Abstr. 94 (1981) 103045d.
[36] S.L. Shapiro, K. Geiger, J. Youlus, L. Freedman, J. Org. Chem. 26 (1961) 3580–3582.
[37] N.E. Cundasawmy, D.B. Maclean, Canad. J. Chem. 50 (1972) 3028–3036.
[38] R.Q. Brewster, F.B. Dains, J. Am. Chem. Soc. 58 (8) (1936) 1364–1366.
[39] R.L. Mital, S.K. Jain, J. Chem. Soc. (c) (1969) 2148–2150.
[40] M. Matsui, Y. Marui, M. Kushida, K. Funabiki, H. Muramastu, K. Shibata, K. Hirota, M. Hosoda, K. Tai, Dyes Pigm. 38 (1998) 57–64.
[41] B.S. Holla, K.N. Poojary, B. Poojary, K.S. Bhat, N.S. Kumari, Ind. J. Chem. 44 B (2005) 2114–2119.
[42] S.N. Dhawan, S. Mor, K. Sharma, A.D. Chawla, A. Saini, S.C. Gupta, Ind. J. Chem. 33 B (1994) 38–42.
[43] H.C. Norman, A.M. Ronald, J. Org. Chem. 26 (1961) 3812–3817.
[44] F.E.M. El-Baih, S.I. Al-Aqeel, O.A. El-Sayed, H.M. Al-Hazimi, J. King Saud. Univ. (Science), Saudi Arabia 18 (1) (2005) 1–17.
[45] H. Sheibani, M.R. Islami, A. Hassanpour, K. Saidi, Phosphorus Sulfur Silicon 3 (2008) 13–20.
[46] H. Sheibani, M.R. Islami, A. Hassanpour, F.A. Hosseininasab, Arkivoc. XV (2006) 68–75.
[47] L. Filak, B.T. Gulbas, Z. Riedl, G.A. Vasko, O. Egyed, I. Yalcin, E.A. Sener, G. Hajos, Acta Chim. Slov. 56 (2009) 622–628.
[48] W.S. Saari, D.W. Cochran, Y.C. Lee, E.L. Cresson, J.P. Springer, M. Williams, J.A. Totaro, G.G. Yarbrough, J. Med. Chem. 26 (1983) 564–569.
[49] K.M. El-Shaieb, J. Sulfur. Chem. 28 (2007) 223–229.
[50] K.R. Scott, M.L. Laws, R.R. Roberts, J.M. Nicholson, United States Patent 5994349 1999.
[51] National Committee for Clinical Laboratory Standards (NCCLs), Standard methods for dilution antimicrobial susceptibility tests for bacteria, which grows aerobically, Nat. Comm. Lab. Stands.Villanova (1982) 242.
[52] C. Hansch, T. Fujita, J. Am. Chem. Soc. 86 (1964) 1616–1626.
[53] C. Hansch, A. Leo, S.H. Unger, K.H. Kim, D. Nikaitani, E.J. Lien, J. Med. Chem. 16 (11) (1973) 1207–1216.
[54] L.B. Kier, L.H. Hall, Molecular Connectivity in Chemistry and Drug Research, Academic Press, New York, 1976.
[55] M. Randic, J. Am. Chem. Soc. 97 (1975) 6609–6615.
[56] A.T. Balaban, Chem. Phys. Lett. 89 (1982) 399–404.
[57] H. Wiener, J. Am. Chem. Soc. 69 (1947) 17–20.
[58] M. Randic, Croat. Chem. Acta 66 (1993) 289–312.
[59] E. Furusjo, A. Svenson, M. Rahmberg, M. Andersson, Chemosphere 63 (2006) 99–108.
[60] A. Golbraikh, A. Tropsha, J. Mol. Graph. Model. 20 (4) (2002) 269–276.
[61] M. Heravi, A. Kyani, J. Chem. Inf. Comput. Sci. 44 (2005) 1328–1335.
[62] L.B. Kier, L.H. Hall, J. Devillers, A.T. Balaban (Eds.), Gordon and Breach Sci. Pub., Amsterdam, 1999, pp. 455–489.
[63] S.P. Gupta, A.N. Kumar, A.N. Nagappa, D. Kumar, S. Kumaran, Eur. J. Med. Chem. 38 (2003) 867–873.
[64] A.D. Pillai, S. Rani, P.D. Rathod, F.P. Xavier, K.K. Vasu, H. Padh, V. Sundarsanam, Bioorg. Med. Chem. 13 (2005) 1275–1283.
[65] S. Bajaj, S.S. Sambi, A.K. Madan, Croat. Chem. Acta 78 (2) (2005) 165–174.
[66] A. Kumar, P. Sharma, V.K. Gurram, N. Rane, Biororg. Med. Chem. Lett. 16 (2006) 2484–2491.
[67] P. Sharma, A. Kumar, M. Sharma, Eur. J. Med. Chem. 41 (2006) 833–840.
[68] S.A. Hatya, E. Aki-sener, B. Tekiner-Gulbas, I. Yildiz, O. Temiz-Arpaci, I. Yalcin, N. Altanlar, Eur. J. Med. Chem. 41 (2006) 1398–1404.
[69] A. Kumar, B. Narasimhan, D. Kumar, Bioorg. Med. Chem. 15 (2007) 4113–4124.
[70] B. Narasimhan, V. Judge, R. Narang, S. Ohlan, R. Ohlan, Bioorg. Med. Chem. Lett. 17 (2007) 5836–5845.
[71] Hyperchem 6.0, Hypercube, Inc., Florida, 1993.
[72] TSAR 3D Version 3.3, Oxford Molecular Limited, 2000.
[73] SPSS for Windows, Version 10.05, SPSS Inc., Bangalore, India, 1999.
[74] K.J. Schaper, Quant. Struct. Act. Relat. 18 (1999) 354–360.